Chemical Reactivity and Structural Investigations on Three Coordinated Chlorostannylenes

Gobbilla Sai Kumar

A dissertation submitted for the partial fulfilment of

BS-MS dual degree in science

Department of Chemical Sciences

Indian Institute of Science Education and Research Mohali

April 2016

Dedicated to my family and friends

for their love and affection

CERTIFICATE OF EXAMINATION

This is to certify that the dissertation titled ***''Chemical Reactivity and Structural Investigations on Three Coordinated Chlorostannylenes''*** submitted by **Mr. Gobbilla Sai Kumar** (Reg. No. MS11047) for the partial fulfilment of BS-MS dual degree programme of the Institute, has been examined by the thesis committee duly appointed by the Institute. The committee finds the work done by the candidate satisfactory and recommends that the report be accepted.

Dr. Angshuman Roy Choudhury Dr. Ujjal K. Gautam Dr. Sanjay Singh

(Supervisor)

Date:

DECLARATION

The work presented in this thesis titled ***''Chemical Reactivity and Structural Investigations on Three Coordinated Chlorostannylenes''*** has been done under the supervision of **Dr. Sanjay Singh** at the Department of Chemical Sciences, Indian Institute of Science Education and Research (IISER), Mohali.

This work has not been submitted in part or full for a degree, a diploma, or a fellowship to any other institute or university. This thesis is a record of work done by me and all other sources has been listed in the bibliography.

Gobbilla Sai Kumar

MS11047

Place:

Date:

In my capacity as a supervisor the above mentioned statements by the candidate are true to the best of my knowledge.

Dr. Sanjay Singh

Associate Professor

Department of Chemical Sciences

Indian Institute of Science Education and Research

Place:

Date:

ACKNOWLEDGEMENT

I would like to thank my supervisor **Dr. Sanjay Singh** who is very helpful throughout my research. I am very thankful to him for teaching me experimental skills and also motivation about research. The confidence and guidance with which he guided the work requires no elaboration. I am very thankful for his continuous support and patience, motivation and immense knowledge throughout my project.

I would like to thank my thesis committee members Prof. Ramesh Kapoor, Dr. Angshuman Roy Choudhury Dr. Ujjal K. Gautam for their valuable inputs and their support. I would like to thank Professor N. Sathyamurthy (Director) for providing the space and all instrumental facilities. I am thankful to Professor K. S. Viswanathan (Head of the Department of Chemical Sciences) for giving suggestions and all the faculty of IISER Mohali for their teaching and constant encouragement.

I would like to acknowledge IISER Mohali for central X-ray diffraction, NMR and HRMS central facilities. I am extremely thankful to the faculty members of IISER Mohali and particularly of the Department of Chemical Sciences. Professor K. S. Viswanathan and all other faculty members of the Department of Chemical Sciences for facilitating the use of various departmental instruments including UV-VIS and FTIR spectrophotometers, particularly XtaLabmini table top X-ray diffractometer.

My sincere thanks to Dr. Billa Prashanth for his help in teaching experimental techniques, handling of solvents and reagents, instrumental techniques and characterization. I would like to thank my lab members Dr. Rishu, Dr. Nagarjuna, Mr. Kuldeep Jaiswal, Mr. Deependra Bawari, Mr. Akhilrag K, Mr. Sabari V. R. and Mr. Anirudha for keeping me motivated and to have maintained a cheerful and peaceful atmosphere in the lab. The discussions in the lab or in the group meetings with these colleagues helped in learning conceptual understanding throughout my final year BS-MS

programme. I want to thank informatics centre for its infrastructure facilities and provide beautiful atmosphere to study. I would like to thank all my MS11 classmates, seniors and juniors for their support and happiness which I shared with them in all these years. I would also like to thank Dr. P. Bapaiah, Dr. P. Visakhi and also all telugu people who are encouraging me throughout my stay in IISER Mohali. I also want to thank my school and intermediate teachers for their support in my early stages of learning.

Finally, I would like to thank my parents, sister and all my relatives for their motivation and support for accomplishing my work. I am very happy to have such a supportive family with me with their love and support throughout my life.

List of Figures and Charts

List of Schemes

List of Tables

Abbreviations

δ	chemical shift
λ	wavelength
$\tilde{\nu}$	wave number
Ar	Aryl
*t*Bu	*tert*-butyl
C	Celsius
calcd.	calculated
d	doublet
dd	doublet of doublet
decomp.	decomposition
EI	electron Impact ionization
Et	Ethyl
Et_2O	diethyl ether
eqv.	equivalents
g	grams
MHz	Mega Hertz
h	hours
*i*Pr	*i*so-propyl
IR	Infrared
J	coupling constant
L	Ligand
M	Metal
M	multiplet
m/z	mass/charge
Mp	melting point
M^+	molecular ion
Me	Methyl
Mes	Mesityl
min.	minutes
MS	mass spectrometry, mass spectra
NMR	nuclear magnetic resonance
ppm	parts per million

q	quartet
R, R', R"	organic substituents
s	singlet
sept	septet
t	triplet
THF	Tetrahydrofuran
V	Volume
Z	number of molecules in the unit cell

CONTENTS

Abstract

The chemistry of low valent group 14 elements has received much attention in recent decades.[1-5] Among them, carbene chemistry has been explored most widely due to their good stability and donor properties. The valency of central atom in metallylenes (R_2M, M = Si, Ge, Sn and Pb) is two. Due to the presence of a vacant p-orbital the metallylenes are highly reactive towards themselves as well as other molecules. They can be stabilized by electron donor atoms such as N, O and Cp* ligands. The N_2P and N_3P_2 types of ligands are also useful scaffolds in stabilizing various four and six membered metal complexes. The substituents on N atoms can be varied to fine tune to offer good donor properties to stabilize both transition as well as main group elements. Various four membered ligands known till to date are amidinates, guanidinates and boramidinates. Among them, amidinates have played an important role in stabilizing low valent metallylenes.

This thesis will describe: The monoanionic [N,N'] ligands based on acyclic N_2P and N_3P_2 backbone that were used to stabilize various four and six membered metal complexes and also to study their reactivity studies. These ligands offer good steric and electronic features. Due to the presence of bulky groups on N atom the ligands have the ability to stop the formation of aggregated molecules. The presence of phosphorous in the ligand is very useful tool to assess the progress of the reactions by ^{31}P NMR spectroscopy.

The synthesis of low valent tin(II) complexes by using these [N,N'] chelating ligands has been undertaken over the known C/N based ligands. The newly synthesized compounds have been characterized by heteronuclear NMR (^{1}H, ^{13}C, ^{31}P, ^{19}F), FT-IR, mass spectrometry and single crystal X-ray diffraction techniques.

1. Introduction

1.1. Basic theory of metallylenes

The chemistry of low valent group 14 elements has received much attention in recent decades.[1-5] Among these, carbene chemistry has been widely explored due to its facile synthesis and good donor ability to coordinate with metal fragments.[6-11] The stability of divalent metal M (II) (M = Si, Ge, Sn, Pb) increases by the increase in principal quantum number (*n*). The formal oxidation state of heavier analogues of carbenes (R_2M:, M = Si, Ge, Sn, Pb) is (II), dichlorostannylene ($SnCl_2$) and dichloroplumbylene ($PbCl_2$) exist as polymeric material.[12] However, in case of germanium, the molecular form exists as $GeCl_2$·dioxane which is stable under inert atmosphere, whereas dihalosilylenes are barely isolable compounds. Simple carbenes prefer triplet as their electronic state but as we go down in group 14 the preference for singlet $(ns)^2(np)^2$ electron configuration increases. The presence of lone pair of electrons heavier metallylenes are nucleophilic in nature and they can stabilize Lewis acids by donating their lone pair of electrons.[13]

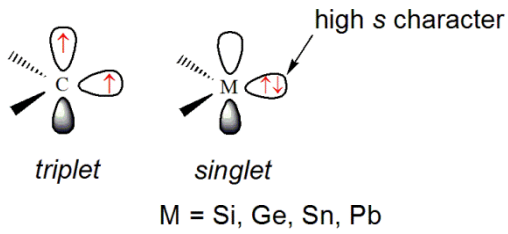

Figure 1. Electronic ground state of simple carbenes and heavier analogues.

However, in group 14 elements the singlet-triplet ΔE_{ST} [ΔE_{ST} = E (triplet) – E (singlet)] energy differences increases as we go down the group and due to this heavier metallylenes exist as singlet in their ground state. Heavier metallylenes have vacant *p*-orbital which can accept electrons and they can be stabilized either by thermodynamic and/or kinetic factors of the substituents on it. Due to the presence of vacant orbital and also lone pair of electrons heavier metallylenes acts as both Lewis acid and Lewis base. Since, the vacant *p*-orbital is highly reactive and can be stabilized by electron donor atoms such as N, O, P and Cp* ligands (Figure 2).[13]

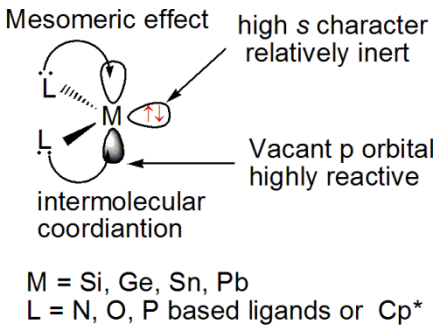

Figure 2. Thermodynamic stabilization of metallylenes.

1.2. [N,N'] chelating ligands based on N-X-N systems (X = C and P) and C_3N_2 backbone

In order to stabilize low valent heavier metallylenes, it is necessary to prepare ligands which have efficient properties such as electronic and steric properties to prevent unwanted reaction to provide kinetic stabilization.[1-5] We have to stabilize heavier metallylenes by using bulky ligands to stabilize them to be isolated and perform further reactions.[14] In this regard we used bulky iminophosphonamide ligand to perform wide variety of reactions. Among various four-membered ligands known till date, amidinates have shown some good electronic and steric properties for stabilization of heavier metallylenes (structure **A**, Figure 3)[15] and in our present work we report iminophosphonamide ligand (structure **B**, Figure 3) which is sterically suitable as well as electron rich to stabilize various metals and shows feasible reactivity.

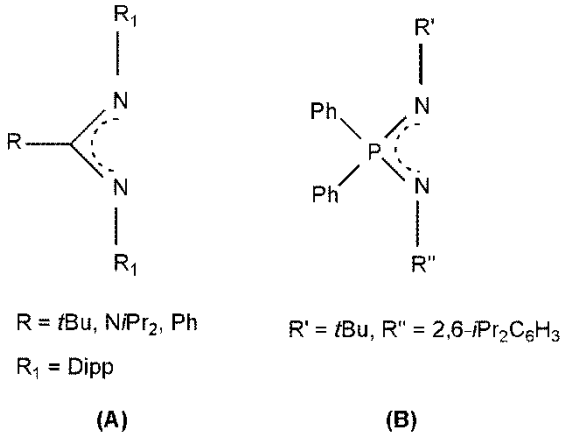

Figure 3. Popular ligands for chemistry with low valent group 14 elements:

amidinate (**A**) and iminophosphonamide (**B**).

Iminophosphonamide ligands offer good steric protection to metallylenes due to the presence of bulky substituents on nitrogen atom. In comparison with amidinate ligand

with N-C-N bite angle of approximately 65-73°, in iminophosphonmide ligand the central phosphorous(V) centers shows a distroted tetrahedral arrangement with a pre determined N-P-N bite angle[16-20] of approximately 108-117° which offers flexible chelates and good stability enabling the chelated metal centre to participate in further chemical reactions.

The N_2P ligand systems had attracted much attention due to its good donor and electronic properties. Another group potential ligands to stabilize different metal complexes are based on C/N type backbone are *β*-diketiminato ligand. The bonding modes of *β*-diketiminato ligand are shown in Chart 3.

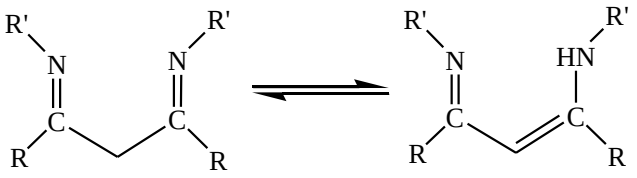

Chart 1. Bonding modes of *β*-diketiminato ligand.

Dias and co-workers used *N*-alkyl-2-(alkylamino)troponiminate (ATI) ligand which is monoanionic and 10*π* electron ring system. The reaction of [(*i*-Pr)$_2$ATI]Li with $SnCl_2$ in an equal molar ratio to form [(*i*-Pr)$_2$ATI]SnCl (Species **I**, Chart 4)[37]. In 2001 Roesky and co-workers synthesized stannylene monochloride [HC{CMeN(2,4-*i*Pr$_2$C$_6$H$_3$)}$_2$]SnCl (Species **II**, Chart 4) by reaction of *β*-diketiminato lithium salt Li(OEt$_2$)[HC{CMeN(2,4-*i*Pr$_2$C$_6$H$_3$)}$_2$] with $SnCl_2$. Single crystal structure of [HC{CMeN(2,4-*i*Pr$_2$C$_6$H$_3$)}$_2$]SnCl[38] shows that the metal centre adopts three-coordinated site which reside in distorted tetrahedral environments with one vertex occupied by a lone pair of electrons.

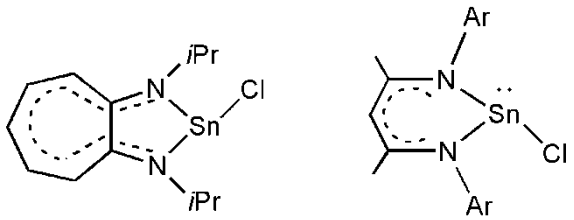

I

Ar = 2,6-*i*PrC$_6$H$_3$

II

Chart 2. Examples of stannylene complexes.

1.3. Heteroleptic complexes of Sn in their low oxidation states and their reactivity studies

Stannylenes are neutral compounds with divalent tin that are considered to be heavier analogues of singlet carbenes. The chemistry of low-valent stannylenes has attracted

much attention in the past few decades and several reviews were reported on it.[22] Lappert and co-workers first isolated and structurally characterized homoleptic stannylene, [Sn{CH(SiMe$_3$)$_2$}$_2$] in 1976,[22] the chemistry of low valent tin compounds has developed widely. Over the past few decades, tremendous efforts had put into the study of homoleptic N-heterocyclic stannylenes. The chemistry of low-valent tin compounds with amidinate ligand has appeared in few reports. These amidinate tin(II) chloride species were synthesized by combining lithium amidinate with $SnCl_2$ by using a variety of bulky substituents on nitrogen atom (Figure 4).[23-25]

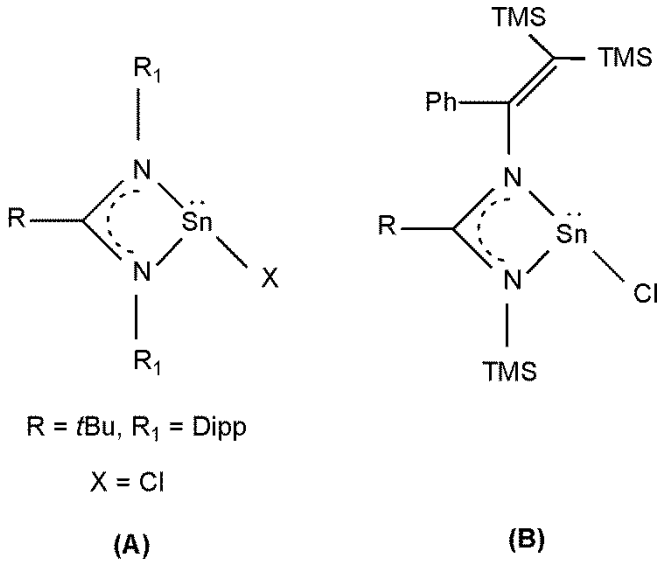

Figure 4. Three-Coordianted chlorostannylene compounds supported by amidinates.

The chlorine atom can be substituted by using heteroatoms such as N and O to synthesize amide alkoxide complexes of tin(II) (Figure 5). The synthesis of amide and alkoxide of tin(II) complexes can be used for further useful reaction which have various applications. For example they can be used to catalyze ring-opening polymerization of lactide very smoothly.

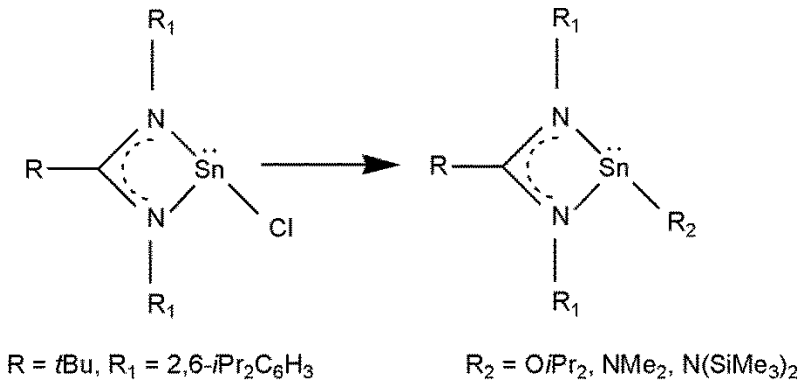

Figure 5. Reaction chemistry of amidinate stannylene chloride.

1.4. Cationic tin complexes

The main class of cations are divided into two categories based on the valency of the charged carbon: carbenium (R_3C^+) and carbonium ions (R_5C^+).[26] Carbenium ions (R_3C^+) bears a positively charged central sp^2 hybridized carbon atom and an unhybridized $2p_z$ orbital with six valence electrons. However, the heavier cations of group 14 elements, R_3E^+ which have been reported as stable species, cations are very difficult to synthesize due to their high reactivity and require protection from any nucleophilic attack. The cations of heavier group 14 elements are divided mainly into two categories, due to their different oxidation state on the metal atom. They are (i) (R_3E^+) and (ii) ($RE:^+$) [E = Si, Ge, Sn and Pb] in which the former class of cations are called tetrylium cation (group 14-tetrel group) which are most common class of cations (Chart 1).

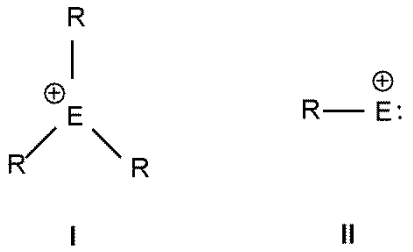

I II

Chart 3. Different classes of heavier group 14 cations.

(i) The generation of R_3Sn^+ have been difficult due to their high electrophilic nature around metal centre.[27] Inability to synthesize heavier group 14 cations is commonly attributed to their high reactivity and low stability. (ii) The other class of cationic species in group 14 elements bears a lone pair of electrons on the metal centre. These cations ($RE:^+$) exhibit nucleophilic ability of carbenes and the electrophilicity of cations. However, there are so many challenges left in chemistry of tin(II) cations.[21] In comparison to neutral species of tin(II) compounds cationic tin complexes are not much explored due to their high reactivity. These cations are very useful for activating small molecules and also few applications in catalytic transformations.[28] These cations can be stabilized in two different ways (i) dehalogenation from $[D\rightarrow EX_2]$ to form $[D\rightarrow EX]^+$ cation; (ii) Another synthetic route to form $[D\rightarrow EX]^+$ (E = Si, Ge, Sn) by the Lewis base promoted ionization of EX_2. The first representative example of stable divalent tin cation, $[(\eta^5\text{-}C_5Me_5)Sn]^+BF_4^-$ (species **I**, Chart 2), was synthesized by Jutzi in 1980. This cation was prepared by reaction of the corresponding stannylenes with HBF_4.[29] Few years later, Schminbaur and co-workers reported Sn(II) cations such as $[\{C_{24}H_{24})Sn(AlCl_4)\}]^+[AlCl_4]^-$ and $[\{C_{24}H_{24})Sn(AlCl_4)\}]^+[Al_2Cl_7]^-$ (species **II**, Chart

2).[30] In 2003 Lambert and co-workers synthesized stable tin(II) cationic species $[Tipp_3Sn]^+[B(C_6F_5)_4]^-$ (Tipp = 2,4,6-*i*$Pr_3C_6H_2$) (species **III**, Chart 2) by the reaction of $Tipp_3SnBr$ with $LiB(C_6F_5)_4$ featuring a three coordinate tin(II) cation.[31] In a similar manner low-valent tin(II) cation $[(\eta^5\text{-}C_5Me_5)Sn]^+[B(C_6F_5)_4]^-$ (species **I**, Chart 2)[32] was prepared by Rhodes and co-workers which has shown an effective co-catalyst in polymerization reactions (Ziegler-Natta).

Lewis base mediated ionization of EX_2 (E = Ge, Sn) has become an useful synthetic approach for $[E\text{-}X]^+$ compounds. Recently, different variety of Lewis bases have been exploited to stabilize tin(II) cations shown below Chart 2. Roesky and co-workers used two equivalents of $SnCl_2$ and 2,6-diacetylpyridinebis(2,6-diisopropylanil) (LB) to isolate cationic tin(II) complex $[(LB)SnCl]^+[SnCl_3]^-$ (LB = 2,6-diacetylpyridinebis(2,6-diisopropylanil)) (species **IV**, Chart 2).[33] Applying a similar synthetic protocol, Jambor and co-workers isolated $[(2\text{-}[C(CH_3)=N(2,6\text{-}iPr_2C_6H_3)]\text{-}6\text{-}(CH_3O)C_6H_3N)SnCl]^+[SnCl_3]^-$ (species **V**, Chart 2)[34] using the diimine ligand. In this complex, ligand is acting as neutral $4e^-$ donor species as [N,N′]- chelating ligand and no Sn←O donation was established and this coordination behaviour of the ligand allowed the stabilization of three-coordinated Sn(II) cations.

Monoanionic bidentate 6π electron backbone system such as β-diketiminate ligand showed excellent capability in stabilizing low valent group 14 cations. In 2011, Fluton and co-workers reported $[CH\{MeCN(2,6\text{-}iPr_2C_6H_3)\}_2Sn]^+[B(C_6F_5)_4]^-$ (species **VI**, Chart 2)[35] by the abstraction of chloride from the corresponding $[CH\{MeCN(2,6\text{-}iPr_2C_6H_3)\}_2]SnCl$ with $LiB(C_6F_5)_4$. In this sequence other tin(II) cation $[CH\{MeCN(2,6\text{-}iPr_2C_6H_3)\}_2Sn]^+[MeB(C_6F_5)_3]^-$ (species **VI**, Chart 2) was also reported.[35]

Very recently, by utilizing the σ- and π-donor capabilities of the sterically demanding ligand carbodiphosphorane, Alcarazo and co-workers have isolated two coordinate $[(Ph_3P)_2C\rightarrow SnCl]_2^{2+}[2(AlCl_4)]^-$ (species **VII**, Chart 2) by the reaction of $(Ph_3P)_2C\cdot SnCl_2$ with an equivalent of $AlCl_3$.[36]

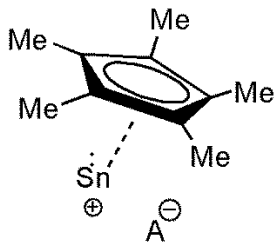

A = BF_4 or $B(C_6F_5)_4$

I

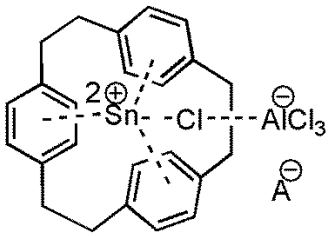

A = $AlCl_4$ or Al_2Cl_7

II

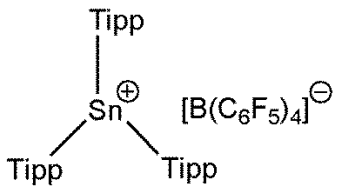

Tipp = 2,4,6-*i*$Pr_3C_6H_2$

III

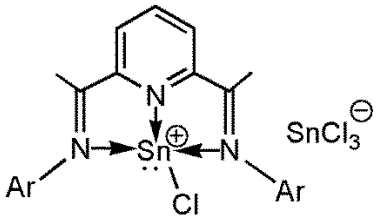

Ar = 2,6-*i*PrC_6H_3

IV

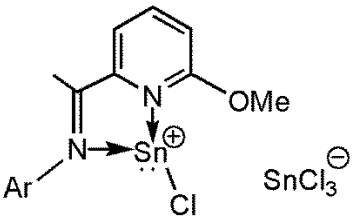

Ar = 2,6-*i*PrC_6H_3

V

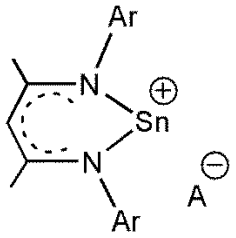

Ar = 2,6-*i*PrC_6H_3

A = $MeB(C_6F_5)_3$; $B(C_6F_5)_4$

VI

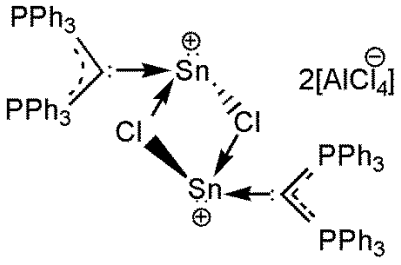

VII

Chart 4. Examples of stannylene cations.

1.5. Aim and scope of present work

The sections 1.1-1.3 describe the importance of ligands in stabilizing group 14 elements in low oxidation states by using N_2C and N_2C_3 as a ligand backbone. The use of halides around the metal centre as useful precursors for studying reactivity studies. In section 1.4 mainly focuses on cationic complexes of tin(II) which are very difficult to isolate due to their low stability and high reactivity. By using these approaches the present work mainly focuses on:

1. Synthesis of chlorostannylene complexes and to study the reactivity studies around the metal centre by using the novel iminophosphonamide and *bis*(phosphinimino)amide ligands.
2. The synthesis of low valent tin cations of group 14 elements in low oxidation state and also to study the stability of these cations.
3. To study the reactivity of chlorogermylene complex by using organic azides.
4. By using the spectroscopic methods such as NMR spectroscopy, IR spectroscopy, mass spectrometry and X-ray analysis for characterization of these newly prepared compounds.

2. Results and Discussion

2.1. Reaction chemistry of stannylene chloride L_ASnCl (1)

2.1.1. *Reaction of $SnCl_2$ with $L_ALi{\cdot}2OEt_2$: Molecular structure of $(L_A)_2Sn$ (2)*

The reaction of $SnCl_2$ with lithium salt $\mathbf{L_A}Li{\cdot}2OEt_2$ ($\mathbf{L_A}$ = [(2,6-*i*$Pr_2C_6H_3N$)(PPh_2)(N*t*Bu)]) which was generated *insitu* by the reaction of $\mathbf{L_AH}$ with *n*BuLi in Et_2O proceeds *via* elimination of lithium chloride LiCl to form the expected product $\mathbf{L_A}SnCl$ **(1)**.[45]

Then the lithium salt, $\mathbf{L_A}Li{\cdot}2OEt_2$ ($\mathbf{L_A}$ = [(2,6-*i*$Pr_2C_6H_3N$)(PPh_2)(N*t*Bu)]) was further reacted with 0.5 equivalent of $SnCl_2$ in diethylether to afford colourless crystalline $\mathbf{(L_A)_2}Sn$ **(2)** (Scheme 1). Complex **2** is stable in inert atmosphere and decomposes easily on exposure to moisture. In ^1H NMR spectrum of compound **2** two sharp singlets at 0.29 & 1.17 ppm for 9 H each. The broad signal around 1.22 & 1.41 ppm was due to presence of *i*Pr group corresponds to 12 H each. Then the septets were seen around 3.76 & 4.02 ppm which is due to C*H*Me_2 pattern corresponds to 2 H each (Fig S1). In $^{31}P\{^1H\}$ NMR spectrum of compound **2** showed a peak around 35.42 ppm (Fig S3).

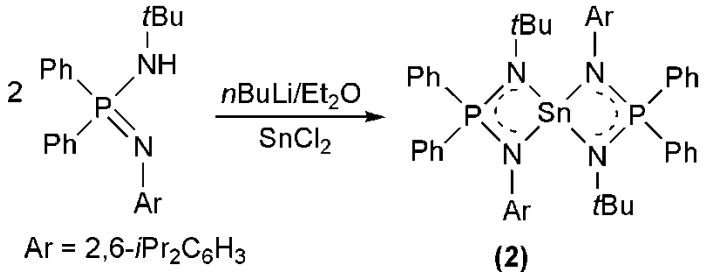

Scheme 1: Synthesis of *bis*-homoleptic iminophosphonamide chelate of tin(II), $\mathbf{(L_A)_2}Sn$ **(2)**.

By maintaining compound **2** in Et_2O solution at overnight in 4 °C resulted in colourless crystals suitable for X-ray structural analysis. Compound **2** crystallizes in the monoclinic crystal system with $P2_1/c$ space group (Figure 6, Table 1). The coordination geometry around Sn(1) can be viewed as distorted saw-horse like arrangement, with N(1) and N(4) in the axial positions and N(2) and N(3) residing in the equitorial plane. Accordingly, the axial Sn(1)-N(1) bond distance is longer (2.517(1) Å) than the Sn(1)-N(2) bond length with 2.243(1) Å. There are several known structures with *bis*-amidinato ligands coordinated to Sn(II), e.g., [{PhC(NSiMe_3)(N*t*Bu)}$_2$Sn][39] and [{PhC(N*t*Bu)$_2$}$_2$Sn].[25] All these reported compounds have more or less distorted saw-horse like coordination with two longer (2.32–2.44 Å) and two shorter Sn-N bonds (2.15–2.27 Å). The anionic charge of both the ligands in compound **2** are delocalized over their respective N-P-N

backbone (with four similar bond lengths P(1)–N(2) 1.606(1), P(1)–N(1) 1.606(2), P(2)–N(3) 1.612(1), P(2)–N(4) 1.599(2) Å).

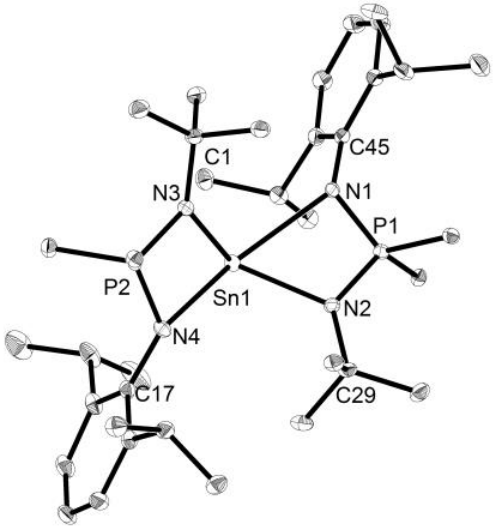

Figure 6. Single crystal X-ray structure of **$(L_A)_2$Sn (2)**. Phenyl rings on the P atoms and hydrogen atoms are omitted for clarity. Thermal ellipsoids have been drawn at 50% probability. Selected bond lengths [Å] and bond angles [°]: P(1)–N(2) 1.606(1), P(1)–N(1) 1.606(2), P(2)–N(3) 1.612(1), P(2)–N(4) 1.599(2), Sn(1)−N(2) 2.243(1), Sn(1)−N(1) 2.517(3), Sn(1)−N(4) 2.517(1), Sn(1)−N(3) 2.234(5), N(4)−C(17) 1.480(1), N(1)−C(45) 1.429(2), N(2)−C(29) 1.496(2), N(3)−C(1) 1.489(2); N(1)−Sn(1)−N(2) 62.67(1), N(3)−Sn(1)−N(4) 62.68(2).

It is to be noted that the bite angles of N-Sn-N in **2** (62.67(1) and 62.68(2)°) are wider than that observed for [{(PhC)(N*t*Bu)$_2$}$_2$Sn][25] (57.75(2)°), [{*t*BuC(N(2,6-*i*Pr$_2$C$_6$H$_3$))$_2$}$_2$Sn][24] (avg 57.27°) and [{MeC(N(2,6-*i*Pr$_2$C$_6$H$_3$))$_2$}$_2$Sn][24] (avg 57.77°)

2.1.2. *Reaction of L_ASnCl (1) with KOtBu: Synthesis of L_ASnOtBu (3)*

An equimolar reaction of **L$_A$**SnCl **(1)** with KO*t*Bu in THF at room temperature resulted in the formation of **L$_A$**SnO*t*Bu (**3**) as a colourless solid (Scheme 2). Compound **3** shows appreciable solubility in solvents such as Et$_2$O, toluene, THF and *n*-hexane and it is stable in solution or solid state under inert atmosphere. Formulation of compound **3** was confirmed by heteronuclear spectroscopic studies and X-ray analysis. The ^{1}H NMR spectrum of **3** showed the characteristic C*H*Me$_2$ pattern, for the 2,6-*i*Pr$_2$C$_6$H$_3$ moiety of the ligand, that appeared as a set of two septets at 3.65 & 4.05 ppm and a set of four doublets for CH*Me$_2$* at 0.08, 0.38, 1.28 and 1.62 ppm. This could be due to two

magnetically non-equivalent *i*Pr groups and the methyl groups of each *i*Pr shows diastereotopic nature. A sharp singlet at 1.36 ppm was assigned to the *t*Bu group on the ligand N and another sharp singlet at 1.83 ppm was assigned to the O*t*Bu group on the Sn centre (Fig S6). The presence of *t*BuO group was further supported by two signals in ^{13}C NMR spectrum (Fig S7) of **3** (33.06 and 76.29 ppm). In $^{31}P\{^{1}H\}$ NMR spectrum compound **3** showed a signal at 38.46 ppm (Fig S8). Mass spectrum of compound **3** suggest the signal at *m/z* = 624.2275 was due to $[M]^+$ (Fig S10).

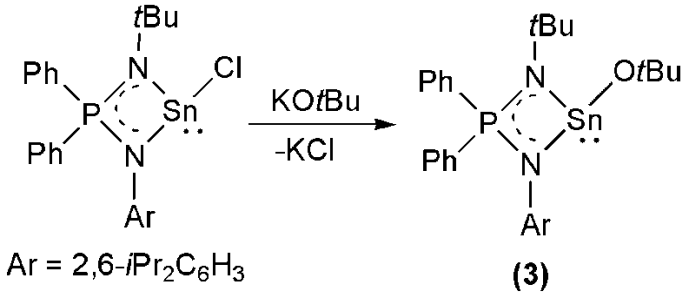

Scheme 2: Synthesis of iminophosphonamide supported tin(II)*tert*-butoxide,

L_ASnO*t*Bu **(3)**.

Maintaining in Et_2O solution of **3** for overnight at 4 °C resulted in colourless single crystals suitable for X-ray structural analysis. Compound **3** crystallizes in the monoclinic crystal system with $P2_1/n$ space group (Figure 7, Table 2). Geometry of the ligand backbone and its coordination to the tin centre is similar to that found in its precursor, **L_A**SnCl **(1)**. The Sn-N bonds in **3** (Sn(1)−N(1) 2.207(1), Sn(1)−N(2) 2.217(2) Å) are slightly shorter than **L_A**SnCl (Sn(1)−N(1) 2.259(2), Sn(1)−N(2) 2.190(1) Å). However, the N-Sn-O bond angles (92.74(5) and 91.58(2)°) are narrower than the N-Sn-Cl angles in **L_A**SnCl (94.40 (1) and 98.37(2)°). It is to be noted that Sn-O distance (2.034(3) Å) in compound **3** is slightly longer than that observed for similar compounds $[PhC(NSiMe_3)_2SnOCPh_3]$ (2.040 Å), $[PhC(NSiMe_2Ph)_2SnOCPh_3]$[40] (2.023 Å), [*t*BuC(NAr)$_2$SnO*i*Pr] (Ar = 2,6-*i*Pr$_2$C$_6$H$_3$)[24] (2.006 Å) show similar Sn-O bond lengths.

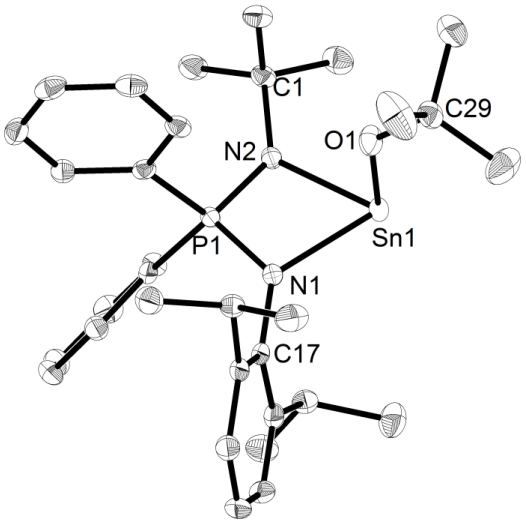

Figure 7. Single crystal X-ray structure of $\mathbf{L_A}$SnO*t*Bu (**3**). All hydrogen atoms have been omitted for clarity. Thermal ellipsoids have been drawn at 50% probability. Selected bond lengths [Å] and bond angles [°]: P(1)–N(1) 1.622(1), P(1)–N(2) 1.610(1), C(1)–N(2) 1.490(2), N(1)–C(17) 1.428(2), Sn(1)−N(1) 2.207(1), Sn(1)−N(2) 2.217(2), Sn(1)−O(1) 2.034(3), O(1)−C(29) 1.419(2); N(1)−Sn(1)−N(2) 67.03(5), N(1)−P(1)−N(2) 98.15(7), Sn(1)−O(1)−C(29) 129.58(2), N(1)−Sn(1)−O(1) 92.74(5), N(2)−Sn(1)−O(1) 91.58(5).

The N-Sn-O angle for compound **3** (92.74(5) and 91.58(5)°) are within the range for these molecules (87.3 to 94.8°).

2.1.3. *Reaction of L_ASnCl (1) with LiN(SiMe$_3$)$_2$ to form L_ASnN(SiMe$_3$)$_2$ (4)*

The reaction of $\mathbf{L_A}$SnCl with LiN(SiMe$_3$)$_2$ in of Et$_2$O at room temperature resulted in the formation of expected product $\mathbf{L_A}$SnN(SiMe$_3$)$_2$ **(4)** as a yellow powder and that is stable under inert atmosphere (Scheme 3). Compound **4** shows good solubility in various solvents such as Et$_2$O, THF and toluene. Further, compound **4** has been characterized by spectroscopic methods.

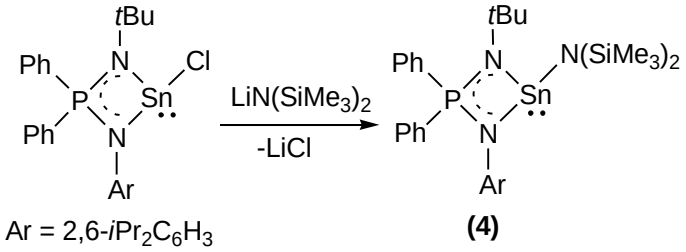

Ar = 2,6-*i*Pr$_2$C$_6$H$_3$ **(4)**

Scheme 3: Synthesis of **L$_A$**SnN(SiMe$_3$)$_2$ **(4)** supported by iminophoshonamide ligand.

In ^{1}H NMR spectrum of compound **4** a singlet around 0.53 ppm due to the presence of N(Si*Me$_3$*)$_2$ moiety on the Sn centre was observed. A sharp singlet at 1.22 ppm was due to *t*Bu group on the ligand N. A septet was observed around 3.59 ppm for the characteristic C*H*Me$_2$ pattern of *i*Pr group (Fig S11). In ^{31}P{^{1}H} NMR spectrum of compound **4** a signal was observed around 32.92 ppm (Fig S13). In the mass spectrum of **4** the signal around *m/z* = 433.2175 was due to the decomposition of compound into ligand (Fig S15).

2.1.4. *Reaction of L$_A$SnCl (1) with Li[Al(OCH(CF$_3$)$_2$)$_4$]: X-ray characterization of L$_A$SnOCH(CF$_3$)$_2$ (6)*

The reaction of **L$_A$**SnCl **(1)** with Li[Al(OCH(CF$_3$)$_2$)$_4$] in THF proceeds by a facile chloride abstraction as LiCl to yield the expected cationic species, *i.e.*, stannylium ion [**L$_A$**Sn]$^+$[Al(OCH(CF$_3$)$_2$)$_4$]$^-$ (**5**) (Scheme 3). The NMR monitoring of the reaction mixture showed the fast conversion of **5** into **L$_A$**SnOCH(CF$_3$)$_2$ (**6)** within 20-30 min. Eventually prolonged storage of compound **5** showed the conversion into neutral complex **L$_A$**SnOCH(CF$_3$)$_2$ (**6)**. Characterization of the crude product showed the expected stannylium ion along with some side product. To ascertain the identity of the side product and its rate of formation the same reaction was carried out in an NMR tube in deuterated solvent and was monitered by *insitu* ^{1}H, ^{19}F and ^{31}P{^{1}H} NMR. Due to high reactivity of stannylium cation **5**, it was not possible to isolate it in the pure form to analyze through spectroscopic and spectrometry techniques. Rapid irreversible conversion of the stannylium ion **5** into the stannylene alkoxide **6** lead to isolation of the latter compound in the pure form. The ^{1}H NMR spectrum of compound **5** showed a peak for CH*Me$_2$* as doublet around 0.28 and 1.04 ppm for 6 H each. Then corresponding septet was observed around 3.42 ppm for 2 H. A sharp singlet was observed around 1.23 ppm for the ligand *t*Bu group. The peak around 4.57 ppm appeared as septet which is due to [Al(OC*H*(CF$_3$)$_2$)$_4$] diastereotopic nature of CF$_3$ groups (Fig S16). The ^{31}P{^{1}H} NMR

spectrum of compound **5** showed a sharp signal at 43.02 ppm (Fig S18). The peak at -77.67 ppm in ^{19}F NMR spectrum (Fig S19) which appeared as a singlet corresponds to [Al(OCH(C*F*$_3$)$_2$)$_4$].

In the ^{1}H NMR spectrum of **6**, characteristic isopropyl pattern for C*H*Me$_2$ appeared as two septets at 3.03 & 4.01 ppm and OC*H*(CF$_3$)$_2$ was observed as septet at 4.65 ppm due to H-F coupling. Three doublets for CH*Me$_2$* were observed at 0.23, 0.52 and 1.31 ppm for three H each, another signal for the fourth methyl group of CH*Me$_2$* appeared as overlapped doublet with *t*Bu group at 1.11 ppm (Fig S20). The ^{31}P{^{1}H} NMR spectrum of compound **6** showed a signal at 46.01 ppm (Fig S22) which is down field shifted as compared to its precursor **L$_A$**SnCl **(1)**. ^{19}F NMR spectrum of this neutral complex **6** also showed two quartets with chemical shifts at -75.5 and -74.9 ppm, respectively (Fig S23). This could be due to diastereotopic CF$_3$ groups on the OCH(CF$_3$)$_2$ moiety. In mass spectrum of compound **6** the signals around *m/z* = 717.1481 and 551.1618 was due to [M]$^+$ and [M-OCH(CF$_3$)$_2$]$^+$ respectively (Fig S25,S26).

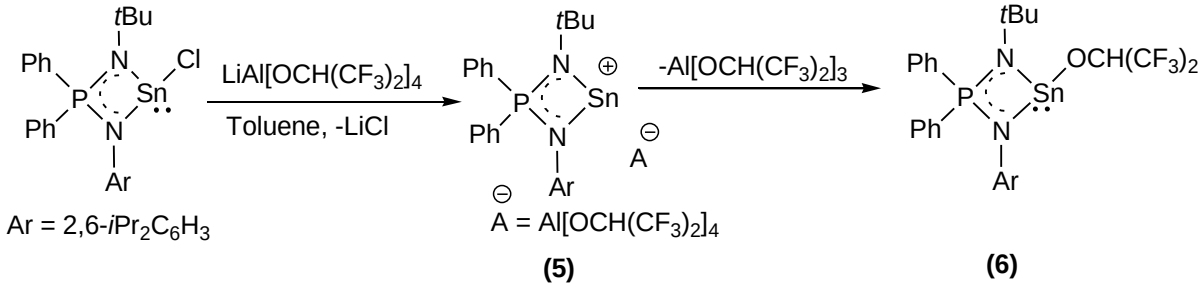

Scheme 4: Synthesis of a stannylium cation **(5)** and its rapid conversion to the neutral complex **(6)**.

Colourless crystals of **6** were obtained from its toluene solution by keeping it at 4 °C. Compound **6** crystallized in monoclinic system with *P*2$_1$/*n* space group (Figure 8, Table 3). The solid state structure reveals that the tin(II) center exhibits pseudo tetrahedral geometry which is build up from iminophosphonamide ligand bonded in a [N,N']-chelate fashion to the tin(II) center and the third site is occupied by OCH(CF$_3$)$_2$ group. The lone pair of electrons occupy fourth position at the tin(II) center.

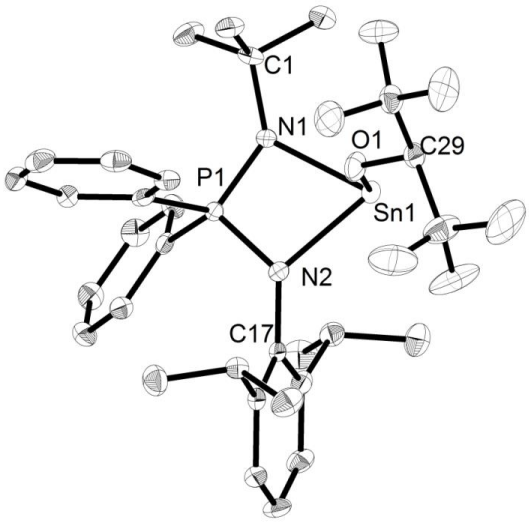

Figure 8. Single crystal X-ray structure of $\mathbf{L_A}SnOCH(CF_3)_2$ (**6**). Thermal ellipsoids have been drawn at 50% probability. Hydrogen atoms are omitted for clarity. Selected bond lengths [Å] and bond angles [°]: P(1)–N(1) 1.613(5), P(1)–N(2) 1.635(3), C(1)–N(1) 1.490(1), N(2)–C(17) 1.436(1), Sn(1)−N(1) 2.187(7), Sn(1)−N(2) 2.182(3), Sn(1)−O(1) 2.082(3), O(1)−C(29) 1.375(1); N(1)−Sn(1)−N(2) 68.20(1), N(1)−P(1)−N(2) 97.90(1), Sn(1)−O(1)−C(29) 121.57(1), N(1)−Sn(1)−O(1) 91.81(1), N(2)−Sn(1)−O(1) 91.29(1).

The Sn-N bond lengths (Sn(1)−N(1) 2.187(7), Sn(1)−N(2) 2.182(3) Å) are comparable to those in $\mathbf{L_A}SnO\mathit{t}Bu$ (**3**) (avg Sn−N 2.212 Å). However, the N-Sn-O bond angles (91.81(1) and 91.29(1)°) are comparable with $\mathbf{L}SnO\mathit{t}Bu$ (**3**) (92.74 (5) and 91.58 (2)°) and smaller than $\mathbf{L_A}SnCl$ (**1**) (94.40(1) and 98.37 (2)°). The Sn-O bond distance in **6** (2.082(3) Å) is comparable with $\mathbf{L_A}SnO\mathit{t}Bu$ (**3**) (2.031(1) Å).

2.1.5. *Reaction of L_BH with $SnCl_2$: X-ray Characterization of L_BSnCl (7)*

The lithium complex $\mathbf{L_B}Li{\cdot}2OEt_2$ which was generated *insitu* by the reaction of $\mathbf{L_BH}$ $[\{(2,6\text{-}\mathit{i}Pr_2C_6H_3N)P(PPh_2)\}_2N]H$ with *n*BuLi was reacted with one equivalent of $SnCl_2$ in Et_2O to form the expected product $\mathbf{L_B}SnCl$ **(7)** in moderate yields proceeds *via* elimination of lithium salt, LiCl (Scheme 5). Compound **7** is highly soluble in solvents such as Et_2O, THF and toluene. It is stable at room temperature under inert atmosphere for weeks. Compound **7** has been characterized by spectroscopic studies and also by X-ray diffraction method. In the ^1H NMR spectrum of compound **7** showed a set of four doublets for $CH\mathit{Me_2}$ around 0.35, 0.77, 1.18 and 1.59 for 6 H each and the corresponding two septets are observed around 3.67 and 4.73 ppm for 2 H each. This could be due to the

presence of magnetically non-equivalent *i*Pr group with diastereotopic nature of two methyl groups on each *i*Pr moiety (Fig S27). In $^{31}P\{^{1}H\}$ NMR spectrum of compound **7** a signal around 14.07 ppm was observed (Fig S29). The mass spectrum of compound **7** showed a signal at *m/z* = 889.3320 and 854.3669 was due to $[M]^+$ and $[M\text{-}Cl]^+$ respectively (Fig 31).

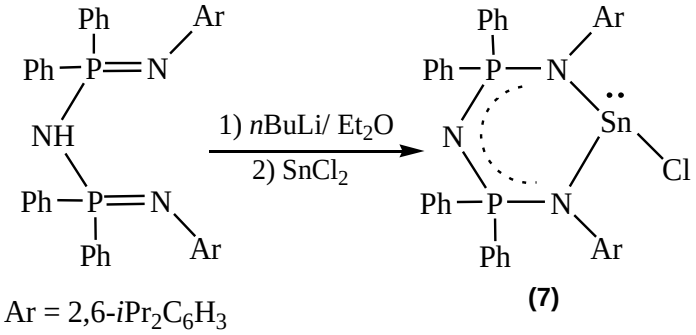

Scheme 5: Synthesis of $\mathbf{L_B}$SnCl **(7)** supported by *bis*(phosphinimino)amide ligand.

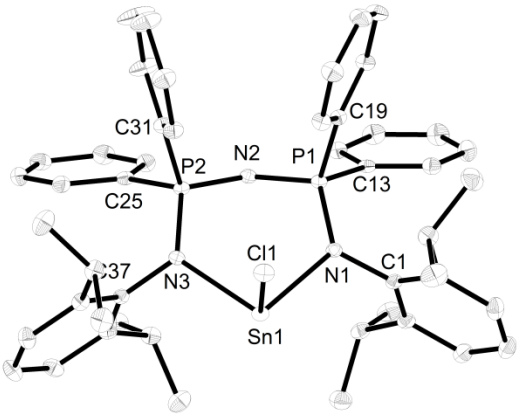

Figure 9. X-ray structure of $\mathbf{L_B}$SnCl **(7)**. All hydrogen atoms are omitted for clarity. Thermal ellipsoids have been drawn at 50% probability. Selected bond lengths [Å] and bond angles [°]: P(1)–N(1) 1.630(3), P(1)–N(2) 1.578(3), P(2)–N(2) 1.580 (4), P(2)–N(3) 1.633(3), Sn(1)–N(1) 2.209(3), Sn(1)–N(3) 2.208(3), Sn(1)–Cl(1) 2.504(2); N(1)–Sn(1)–N(3) 99.18(1), Cl(1)–Sn(1)–N(1) 95.02(1), Cl(1)–Sn(1)–N(3) 93.55(2).

Maintaining a solution of **7** in Et_2O at −30 °C overnight resulted in the formation of colourless crystal of compound **7** suitable for X-ray analysis. Compound **7** crystallizes in triclinic system with *P*$\bar{1}$ space group (Figure 9, Table 4). The geometry around the ligand

backbone of compound **7** is similar to that found in [HC-(C(Me)N-2,6-*i*Pr$_2$C$_6$H$_3$)$_2$)]SnCl.[38] The Sn-N bond lengths in compound **7** are slightly longer than the corresponding distance in [HC-(C(Me)N-2,6-*i*Pr$_2$C$_6$H$_3$)$_2$)]SnCl (2.180(2) and 2.185(2) Å), but on comparing with **L$_A$**SnCl **(1)** the bond lengths are slightly shorter (avg 2.224 Å). However the N-Sn-N bond angle of compound **7** is wider than corresponding angle in, [HC-(C(Me)N-2,6-*i*Pr$_2$C$_6$H$_3$)$_2$)]SnCl[38] (85.21(8)°) and **L$_A$**SnCl **(1)** (67.20(6)°) it indicates the strong coordination of N-Sn-N in compound **7**. This is attributed due to strong donor properties of P=N compared to C=N.

2.1.6. *Reaction of L$_B$SnCl (7) with Li[Al(OCH(CF$_3$)$_2$)$_4$] to form [L$_B$Sn]$^+$[Al(OCH(CF$_3$)$_2$)$_4$]$^-$ (8)*

The complex [**L$_B$**Sn]$^+$[Al(OCH(CF$_3$)$_2$)$_4$]$^-$ **(8)** was formed by the reaction of one equivalent of **L$_B$**SnCl **(7)** with Li[Al(OCH(CF$_3$)$_2$)$_4$] in the presence of THF which was allowed to stir overnight at room temperature. Compound **8** was characterized by spectroscopic techniques.

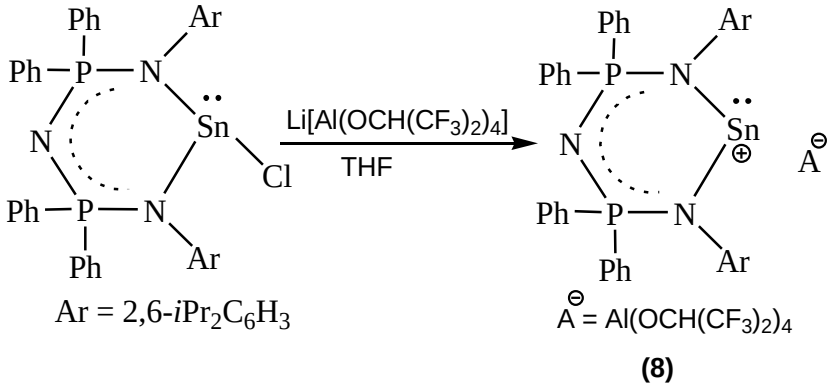

Scheme 6: Synthesis of [**L$_B$**Sn]$^+$[Al(OCH(CF$_3$)$_2$)$_4$]$^-$ **(8)** complex.

The ^{1}H NMR spectrum of compound **8** showed characteristic isopropyl patterns that appeared as two doublets around 0.46 and 0.79 ppm for CH*Me$_2$* each for 6 H. The peak at 0.79 ppm was due to CH*Me$_2$* moiety for 12 H. This pattern is due to magnetically non-equivalent *i*Pr groups with diastereotopic methyl groups. Two septets were observed around 2.87 and 3.30 ppm due to C*H*Me$_2$ moiety of the *i*Pr group (Fig S32). In the ^{31}P{^{1}H} NMR spectrum of compound **8** a sharp peak at 18.26 ppm was observed (Fig S34). Further monitoring of ^{31}P{^{1}H} NMR spectrum the peak around 16.24 ppm was attributed due to the conversion of **8** into neutral complex tin alkoxide **L$_B$**SnOCH(CF$_3$)$_2$. This is due to the fact that cation complexes are labile and this type of exchange is

observed in Lewis acid mediated synthesis of cationic tin species both in compound **4** and **8**. In ^{19}F NMR spectrum a sharp peak appeared around -76.37 ppm (Fig 35).

2.1.7. *Oxidation of L_AGeCl (9) with 2,4,6-$Me_3C_6H_2N_3$ to form $L_AGe(=NAr)Cl$ [Ar=2,4,6- $Me_3C_6H_2$ (10)]*

The reaction of lithium complex $\mathbf{L_A}Li\cdot 2OEt_2$ was generated *insitu*, with one equivalent of $GeCl_2$.dioxane in presence of Et_2O to form the expected product $\mathbf{L_A}GeCl$.[47] When germylene chloride was reacted with the azide 2,4,6-$Me_3C_6H_2N_3$ in toluene, oxidation of germylene occurred leading to the formation of $\mathbf{L_A}Ge(=NAr)Cl$ [Ar = 2,4,6-$Me_3C_6H_2$] **(7)** (Scheme 7). Compound **10** was characterized by NMR spectroscopy and mass spectrometry.

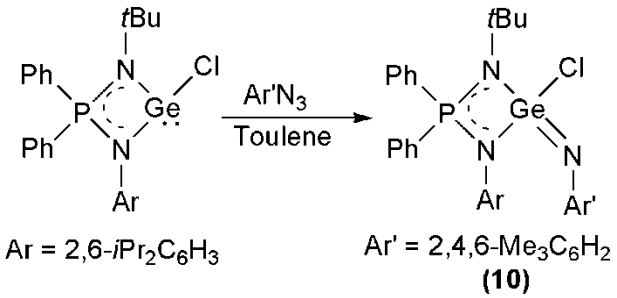

Scheme 7: Synthesis of $\mathbf{L_A}Ge(=NAr)Cl$ [Ar = 2,4,6-$Me_3C_6H_2$] **(10)**

In the ^1H NMR spectrum, compound **10** showed two doublets for CH*Me*$_2$ at 0.12 and 0.99 ppm for six H each and broad signal for C*H*Me_2 was observed at 3.29 ppm for two H. A singlet appeared for *t*Bu at 1.37 ppm and singlet for *p-Me* and *o-Me* were observed at 2.22 and 2.54 ppm respectively, for three and six H each (Fig S38). The $^{31}P\{^1H\}$ NMR spectrum of compound **10** showed a signal at 30.49 ppm (Fig S40). In mass spectrum of **10** the signal around *m/z* = 566.2852 was due to $[M-(C_9H_2NCl)]^+$ (Fig S42).

3. Experimental Section:

3.1. General procedure

All manipulations and handling of reagents were carried out under an inert atmosphere (dry nitrogen or argon) using standard Schlenk techniques or a glovebox where O_2 and H_2O level was maintained usually below 0.1 ppm. All glassware was dried at 150 °C in an oven for at least 20 h prior to use. Toluene, tetrahydrofuran, diethyl ether and *n*-hexane were purified with the M-Braun solvent drying system prior to use.

3.2. Physical measurements

The ^{1}H, ^{13}C, $^{31}P\{^{1}H\}$ and ^{19}F NMR spectra were recorded with a Bruker 400 MHz spectrometer with TMS, H_3PO_4 (85%) and $CFCl_3$ respectively, as the external reference and chemical shifts are reported in ppm. Downfield shifts relative to the reference are quoted positive; upfield shifts are assigned negative values. Heteronuclear NMR spectra were recorded ^{1}H decoupled. Deuterated NMR solvents benzene−d_6, toluene−d_8, and THF–d_8 were dried over Na and $CDCl_3$ was dried over 4 Å molecular sieves. High resolution mass spectra were recorded on a Waters SYNAPT G2−S. IR spectra of the compounds were recorded in the range 3500–400 cm^{-1} using a Perkin Elmer Lambda 35-spectrophotometer as nujol mull between KBr plates. The absorptions of various functional groups are assigned and other absorptions (moderate to very strong) are only listed. Melting points were measured in sealed capillaries on a Büchi B–540 melting point instrument.

Single crystal X-ray diffraction data of compound **3** was collected on a Bruker *AXS KAPPA APEX-II* CCD diffractometer (Monochromatic MoKα radiation) equipped with Oxford cryosystem 700 plus at 100 K. Data collection and unit cell refinement for the data sets were done using the Bruker APPEX-II suite, data reduction and integration were performed using SAINTV 7.685A (Bruker AXS, 2009)[48] and absorption corrections and scaling were done using SADABSV2008/1 (Bruker AXS, 2009).[48] The crystal structures were solved by using OLEX2 package using SHELXS-97 and the structures were refined using SHELXL-97 2008.47.[50] Single crystal X-ray diffraction data of **2, 6** and **7** were collected using a Rigaku XtaLAB mini diffractometer equipped with Mercury375M CCD detector. The data were collected with graphite monochromatic MoKα radiation (λ = 0.71073 Å) at 100.0(2) K using scans. During the data collection the detector distance was 50 mm (constant) and the detector was placed at 2θ = 29.85° (fixed) for all the data

sets. The data collection and data reduction were done using Crystal Clear suite.[43] The space group determination was done using Olex2.[48] The structures were solved by direct method and refined by full-matrix least-squares procedures using the SHELXL-97[50] software package using Olex2 suite. All non-hydrogen atoms were refined anisotropically. Hydrogen atoms were fixed at geometrically calculated positions and were refined using riding model. Diamond version 2.1d was used to generate graphics for the X-ray structures. The crystal data for all compounds along with the final residuals and other pertaining details are tabulated in Tables **1**–**4**.

3.3. Starting materials

All chemicals used in this work were purchased from commercial sources and were used without further purification. [(2,6-*i*Pr$_2$C$_6$H$_3$N)P(Ph$_2$)(N*t*Bu)]H[53], [{(2,6-*i*Pr$_2$C$_6$H$_3$N)P(PPh$_2$)}$_2$N]H[53], Ph$_2$PNH*t*Bu[52], 2,6-*i*Pr$_2$C$_6$H$_3$N$_3$[51], 2,4,6-Me$_3$C$_6$H$_2$N$_3$[44], [(2,6-*i*Pr$_2$C$_6$H$_3$N)P(Ph$_2$)(N*t*Bu)]SnCl[45,53], [(2,6-*i*Pr$_2$C$_6$H$_3$N)P(Ph$_2$)(N*t*Bu)]GeCl[46] and Li[Al(OCH(CF$_3$)$_2$)$_4$][47] were prepared by literature procedures.

3.4. Synthesis of compounds 2, 3, 4, 5, 6, 7, 8 and 10

3.4.1. *Synthesis of (L$_A$)$_2$Sn: [L$_A$ = (2,6-iPr$_2$C$_6$H$_3$N)(PPh$_2$)(NtBu)] (2)*

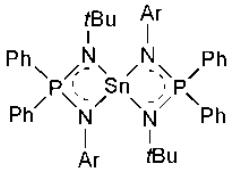

A solution of **L$_A$H** (0.86 g, 2.00 mmol) in Et$_2$O (30 mL) was cooled to -78 °C and *n*BuLi (1.50 mL, 1.6 M in hexane) was added to it. The mixture was allowed to stir for 3 hours at room temperature. The resultant solution was added to a solution of SnCl$_2$ (0.22 g, 1.16 mmol) in Et$_2$O (15 mL) at -78 °C. The compound was allowed to stir for overnight at room temperature. The insoluble LiCl was removed by filtration and the solvent was partially reduced. The solution was kept at 4 °C to obtain colourless crystals of **2**. **^{1}H NMR** (400 MHz, C$_6$D$_6$): δ = 0.29 (s, 9 H, *t*Bu), 1.17 (s, 9 H, *t*Bu), 1.22 (br, 12 H, C*H*M*e*$_2$), 1.41 (br, 12 H, C*H*M*e*$_2$), 3.76 (sept, $^3J_{H\text{-}H}$ = 6.8 Hz, 2 H, C*H*Me$_2$), 4.02 (sept, $^3J_{H\text{-}H}$ = 6.4 Hz, 2 H, C*H*Me$_2$), 6.94-7.02 (m, 7 H, Ar), 7.04-7.13 (m, 4 H, Ar), 7.29-7.37 (m, 4 H, Ar), 7.44-7.50 (m, 3 H, Ar), 7.56-7.64 (m, 5 H, Ar), 7.76-7.85 (m, 3 H, Ar) . **^{13}C NMR** (100 MHz, C$_6$D$_6$): δ = 16.0, 24.7, 29.3, 32.4, 52.8, 66.2, 123.6, 128.8, 131.1, 132.4, 132.5, 133.8. **^{31}P{^{1}H} NMR** (162 MHz, C$_6$D$_6$): δ = 35.42. **Mass Spectrum** (AP, +ve), *m/z* = 549.1405 [M-(2H+C$_{28}$H$_{36}$N$_2$P)]$^+$. **IR** (Nujol, cm^{-1}): 2922, 2725, 1599, 1456, 1375, 1303, 1072, 1027, 959, 759, 724, 691, 525, 466.

3.4.2. *Synthesis of L_ASnOtBu (3)*

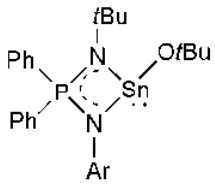

To a solution of **L_A**SnCl **(1)** (0.58 g, 1.00 mmol) in THF (10 mL) was added to a solution of KO*t*Bu (0.11 g, 1.00 mmol) in THF (10 mL) at room temperature and stirred for overnight. The solvent was evaporated under vacuum and the residue was extracted with Et_2O. Keeping the solution at 4 °C affords colourless needle crystals of **3**. Yield: (0.38 g, 67 %). Mp: 100.5 °C. **^{1}H NMR** (400 MHz, C_6D_6): δ = 0.08 (d, $^3J_{H\text{-}H}$ = 6.8 Hz, 3 H, CH*Me*$_2$), 0.38 (d, $^3J_{H\text{-}H}$ = 6.8 Hz, 3 H, CH*Me*$_2$), 1.28 (d, $^3J_{H\text{-}H}$ = 6.8 Hz, 3 H, CH*Me*$_2$), 1.36 (s, 9 H, *t*Bu), 1.62 (d, $^3J_{H\text{-}H}$ = 6.8 Hz, 3 H, CH*Me*$_2$), 1.83 (s, 9 H, O*t*Bu), 3.65 (sept, $^3J_{H\text{-}H}$ = 6.8 Hz, 1 H, *CH*Me$_2$), 4.05 (sept, $^3J_{H\text{-}H}$ = 6.8 Hz, 1 H, *CH*Me$_2$), 6.92-6.98 (m, 4 H, Ar), 6.99-7.05 (m, 5 H, Ar), 7.51-7.57 (m, 2 H, Ar), 8.21-8.28 (m, 2 H, Ar). **^{13}C NMR** (100 MHz, C_6D_6): δ = 24.7, 25.2, 26.6, 28.5, 29.4, 31.3, 33.1, 33.3 (d, $J_{C\text{-}P}$ = 5.6 Hz), 55.5, 76.3, 124.5 (d, $J_{C\text{-}P}$ = 2.6 Hz), 125.7 (d, $J_{C\text{-}P}$ = 2.6 Hz), 126.1 (d, $J_{C\text{-}P}$ = 102.8 Hz), 127.3 (d, $J_{C\text{-}P}$ = 2.8 Hz), 128.8, 129.2 (d, $J_{C\text{-}P}$ = 12.8 Hz), 131.0 (d, $J_{C\text{-}P}$ = 2.8 Hz), 132.5 (d, $J_{C\text{-}P}$ = 98.7 Hz), 132.4 (d, $J_{C\text{-}P}$ = 9.6 Hz), 132.5 (d, $J_{C\text{-}P}$ = 1.4 Hz), 133.3 (d, $J_{C\text{-}P}$ = 10.0 Hz), 135.3 (d, $J_{C\text{-}P}$ = 11.5 Hz), 149.3 (d, $J_{C\text{-}P}$ = 4.5 Hz), 151.0 (d, $J_{C\text{-}P}$ = 4.4 Hz). **^{31}P{^{1}H} NMR** (162 MHz, C_6D_6): δ = 38.46. **Mass Spectrum** (AP, +ve), *m/z* = 624.2275 $[M]^+$. **IR** (Nujol, cm^{-1}): 2955, 2924, 2854, 1589, 1459, 1438, 1378, 1364, 1326, 1257, 1218, 1200, 1131, 1109, 955, 906, 839, 784, 748, 699.

3.4.3. *Synthesis of L_ASnN(SiMe$_3$)$_2$ (4)*

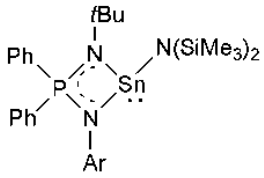

To a solution of **L_A**SnCl **(1)** (0.58 g, 1.00 mmol) in Et_2O (10 mL) was added to a solution of $LiN(SiMe_3)_2$ (0.2 mL, 1.00 mmol) in Et_2O (10 mL) at room temperature and stirred for overnight. The solvent was evaporated under vacuum and the residue was extracted with *n*hexane. Keeping the solution at 4 °C affords colourless powder **4**. Yield: (0.38 g, 65 %). Mp: 85 °C. **^{1}H NMR** (400 MHz, C_6D_6): δ = 0.53 (s, 18 H, N(Si*Me*$_3$)$_2$), (CH*Me*$_2$ group is not observed), 1.22 (s, 9 H, *t*Bu), 3.59 (sept, $^3J_{H\text{-}H}$ = 6.8 Hz, 2 H, *CH*Me$_2$), 6.93-7.03 (broad, 8 H, Ar), 7.54-7.66 (broad, 2 H, Ar), 7.72-7.88 (broad, 3 H, Ar). **^{13}C NMR** (100 MHz, C_6D_6): δ = 24.7, 28.8, 29.4, 34.9 (d, $J_{C\text{-}P}$ = 7.14 Hz), 53.4, 123.7, 124.5 (d, $J_{C\text{-}P}$ = 2.5 Hz), 125.1 (d, $J_{C\text{-}P}$ = 3.8 Hz), 129.0, 131.0, 131.1, 132.4, 132.5, 133.4, 133.8, 142.4, 142.5. **^{31}P{^{1}H} NMR** (162 MHz, C_6D_6): δ = 32.92. **Mass Spectrum**

(+ve ion, EI), *m/z* = 433.2175*. **IR** (Nujol, cm^{-1}): 3055, 2957, 2924, 2856, 2723, 1590, 1458, 1376, 1300, 1255, 1220, 1181, 1107, 1025, 931, 882, 842, 749, 722, 697.

3.4.4. *Synthesis of $[L_ASn]^+[Al(OCH(CF_3)_2)_4]^-$ (5) and $L_ASn[OCH(CF_3)_2]$ (6)*

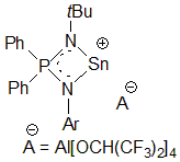

The reaction of $\mathbf{L_A}$SnCl (0.05 g, 0.1 mmol) with Li[Al(OCH(CF_3)$_2$)$_4$] (0.07 g, 0.1 mmol) in presence of THF to offered the expected product [$\mathbf{L_A}$Sn]$^+$[Al(OCH(CF_3)$_2$)$_4$]$^-$ **(5)**. The reaction was performed *insitu* in NMR tube.

Spectroscopic characterization of *$[L_ASn]^+[Al(OCH(CF_3)_2)_4]^-$ (5)*

^{1}H NMR (400 MHz, THF): δ = 0.28 (broad, 6 H, CH*Me*$_2$), 1.04 (d, $^3J_{H\text{-}H}$ = 6.4 Hz, 6 H, CH*Me*$_2$), 1.23 (s, 9 H, *t*Bu), 3.42 (sept, $^3J_{H\text{-}H}$ = 6.8 Hz, 2 H, *CH*Me$_2$), 4.57 (sept, $^3J_{H\text{-}F}$ = 6.0 Hz, 4 H, C*H*(CF_3)$_2$, 6.81-6.96 (broad, 3 H, Ar), 7.29-7.65 (m, 6 H, Ar), 7.77-8.09 (m, 4 H, Ar). **^{13}C NMR** (100 MHz, THF): δ = 22.2, 23.4, 27.9, 33.4 (d, $J_{C\text{-}P}$ = 6.7 Hz), 52.5, 70.9 (d, $J_{C\text{-}P}$ = 32.2 Hz), 121.6 (d, $J_{C\text{-}P}$ = 2.2 Hz), 122.0, 123.1 (d, $J_{C\text{-}P}$ = 2.4 Hz), 124.1, 127.6, 127.7, 128.0, 128.1, 131.6, 131.7, 131.8 (d, $J_{C\text{-}P}$ = 2.4 Hz), 132.9. **^{31}P{^{1}H} NMR** (162 MHz, THF): δ = 43.02. **^{19}F NMR** (376 MHz, THF): δ = -77.67.

Spectroscopic characterization of *$L_ASnOCH(CF_3)_2$ (6)*

*Alternative synthesis of **(6)**:*

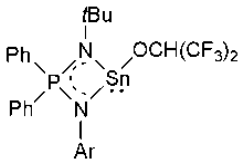

The reaction of $\mathbf{L_A}$SnCl (0.58 g, 1 mmol) with LiOCH(CF_3)$_2$ (0.1 mL, 1 mmol) in presence of Et_2O at room temperature and stirred for 12 h to afford $\mathbf{L_A}$Sn[OCH(CF_3)$_2$]. Then the salt LiCl was filtered out and evaporated under vacuum.

Yield: (0.15 g, 58 %). Mp: 125 °C (decomp). **^{1}H NMR** (400 MHz, C_6D_6): δ = 0.23 (d, $^3J_{H\text{-}H}$ = 6.8 Hz, 3 H, CH*Me*$_2$), 0.52 (d, $^3J_{H\text{-}H}$ = 6.8 Hz, 3 H, CH*Me*$_2$), 1.11 (12 H, *t*Bu overlapped with CH*Me*$_2$), 1.31 (d, $^3J_{H\text{-}H}$ = 6.8 Hz, 3 H, CH*Me*$_2$), 3.03 (sept, $^3J_{H\text{-}H}$ = 6.8 Hz 1 H, *CH*Me$_2$), 4.01 (sept, $^3J_{H\text{-}H}$ = 6.8 Hz, 1 H, *CH*Me$_2$), 4.65 (sept, $^3J_{H\text{-}F}$ = 6.8 Hz, 1 H, *CH*(CF_3)$_2$), 6.76-6.81 (m, 1 H, Ar), 6.87-6.95 (m, 2 H, Ar), 7.12-7.18 (m, 6 H, Ar), 7.41-7.48 (m, 2 H, Ar), 8.34 (broad, 2 H, Ar). **^{13}C NMR** (100 MHz, C_6D_6): δ = 21.7, 22.9, 24.7, 25.4, 28.6, 29.2, 34.1, 34.3, 52.9, 71.7 (q, $J_{C\text{-}F}$ = 33.0 Hz), 73.0 (q, $J_{C\text{-}F}$ = 33.0 Hz), 124.6 (d, $J_{C\text{-}P}$ = 2.5 Hz), 124.7 (dd, $J_{C\text{-}P}$ = 150 & 3.2 Hz), 126.0, 129.3 (d, $J_{C\text{-}P}$ = 77.3 Hz), 132.0 (d, $J_{C\text{-}P}$ = 2.6 Hz), 132.6 (d, $J_{C\text{-}P}$ = 9.6 Hz), 134.7 (d, $J_{C\text{-}P}$ = 11.4 Hz), 135.7 (d, $J_{C\text{-}P}$ = 93.9 Hz), 137.5 (d, $J_{C\text{-}P}$ = 2.4 Hz), 138.2, 146.8 (d, $J_{C\text{-}P}$ = 5.1 Hz), 148.8 (d, $J_{C\text{-}P}$ =

5.0 Hz). **^{31}P{^{1}H} NMR** (162 MHz, C_6D_6): δ = 46.01. **^{19}F NMR** (376 MHz, C_6D_6): δ = -75.5 (q, $J_{F\text{-}F}$ = 9.41 Hz), -74.9 (q, $J_{F\text{-}F}$ = 9.41 Hz). **Mass Spectrum** (AP, +ve), *m/z* = 717.1481 $[M]^+$, 551.1618 $[M\text{-}OCH(CF_3)_2]^+$. **IR** (Nujol, cm^{-1}): 2948, 2923, 2854, 1634, 1586, 1456, 1376, 1303, 1256, 1218, 1197, 1181, 1113, 1057, 995, 843, 743, 695.

3.4.5. *Synthesis of L_BSnCl (7)*

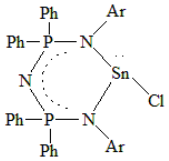

A solution of [{(2,6-*i*Pr$_2$C$_6$H$_3$N)P(PPh$_2$)}$_2$N]H (**L_BH**) (1.47 g, 2.0 mmol) in Et_2O (20 mL) was cooled to −78°C. To it was added *n*BuLi (1.25 mL, 2.0 mmol, 1.6 м in hexane) and was allowed to come to room temperature and stirred for 3 h. The resultant solution was added to a solution of $SnCl_2$ (0.46 g, 2.0 mmol) in Et_2O at −78 °C. The mixture was slowly warmed to room temperature and stirred for further 10 h. The precipitate was filtered, and the solvent was partially reduced (*ca.* 15 mL). Keeping the solution at −30 °C for overnight afforded colorless crystals of **7**, which was suitable for X-ray diffraction analysis. Yield: (0.38 g, 63 %). Mp: 160°C. **^{1}H NMR** (400 MHz, C_6D_6): δ = 0.35 (d, $^{3}J_{H\text{-}H}$ = 4.5 Hz, 6 H, CH*Me*$_2$), 0.77 (d, $^{3}J_{H\text{-}H}$ = 4.5 Hz, 6 H, CH*Me*$_2$), 1.18 (d, $^{3}J_{H\text{-}H}$ = 4.2 Hz, 6 H, CH*Me*$_2$) 1.59 (d, $^{3}J_{H\text{-}H}$ = 4.5 Hz, 6 H, CH*Me*$_2$), 3.67 (broad, 2 H, *CH*Me$_2$), 4.73 (broad, 2 H, *CH*Me$_2$), 6.82−6.88 (m, 6 H, Ar), 6.89−6.96 (m, 9 H, Ar), 7.06−7.13 (m, 3 H, Ar), 7.59−7.65 (m, 4 H, Ar), 7.88−7.96 (m, 4 H, Ar). **^{13}C NMR** (100 MHz, C_6D_6): δ = 22.8, 24.4, 27.8, 28.4, 29.1, 29.6, 123.8, 124.7, 125.4, 126.4 (d, $J_{C\text{-}P}$ = 2.9 Hz), 127.6 (d, $J_{C\text{-}P}$ = 13.2 Hz), 128.0, 130.5 (d, $J_{C\text{-}P}$ = 2.7 Hz), 130.7, 131.3 (d, $J_{C\text{-}P}$ = 2.6 Hz), 134.6, 135.8, 138.3 (d, $J_{C\text{-}P}$ = 5.2 Hz), 148.5, 149.9. **^{31}P{^{1}H} NMR** (162 MHz, C_6D_6): δ = 14.1. **Mass spectrum** (+ve ion, EI), *m/z* = 889.3320 $[M]^+$, 854.3669 $[M-Cl]^+$. **IR** (Nujol, cm^{-1}) $\tilde{\nu}$: 2954, 2923, 2856, 2721,1458, 1378, 1310, 1257, 1236, 1178, 1109, 1047, 983, 789, 720. 593.

3.4.6. *Synthesis of $[L_BSn]^+[Al(OCH(CF_3)_2)_4]^-$ (8)*

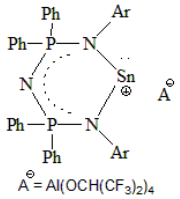

The reaction of **L_BSnCl (7)** (0.89 g, 1 mmol) with Li[Al(OCH(CF$_3$)$_2$)$_4$] (0.71 g, 1 mmol) in presence of THF at room temperature and stirred for 12 h to offered the expected product **$[L_BSn]^+$**[Al(OCH(CF$_3$)$_2$)$_4$]$^-$ **(8)**. Then the salt LiCl was filtered out and the solvent evaporated under vaccum. **^{1}H NMR** (400 MHz, C_6D_6): δ = 0.46 (d, $^{3}J_{H\text{-}H}$ = 6.8 Hz, 6 H, CH*Me*$_2$), 0.79 (d, $^{3}J_{H\text{-}H}$ = 6.8 Hz, 12 H, CH*Me*$_2$), 1.09 (d, $^{3}J_{H\text{-}H}$ = 6.8 Hz, 6 H, CH*Me*$_2$), 2.87 (sept, $^{3}J_{H\text{-}H}$ = 6.8 Hz, 2 H, *CH*Me$_2$), 3.30 (sept, $^{3}J_{H\text{-}H}$ = 6.8 Hz, 2 H, *CH*Me$_2$), 4.90-4.99 (m, 4 H, O(CH(CF$_3$)$_2$)$_4$),

6.85-6.89 (m, 1 H, Ar), 6.90-6.96 (broad, 7 H, Ar), 6.99-7.04 (broad, 8 H, Ar), 7.09-7.14 (broad, 4 H, Ar), 7.17-7.22 (broad, 2 H, Ar), 7.29-7.38 (broad, 4 H, Ar). **^{13}C NMR** (100 MHz, C_6D_6): δ = 21.7, 22.3, 23.5, 28.6, 29.3, 29.5, 72.1 (q, O*C*H$(CF_3)_2$, $J_{C\text{-}F}$ = 33.0 Hz), 122.3 (broad, OCH(*C*F$_3$)$_2$), 124.9, 125.7, 126.0, 127.3 (d, $J_{C\text{-}P}$ = 3.7 Hz), 129.0, 129.4 (vtr, $J_{C\text{-}P}$ = 7.0 & 13.9 Hz), 131.4 (broad), 131.9 (vtr, $J_{C\text{-}P}$ = 5.6 & 11.4 Hz), 132.4 (d, $J_{C\text{-}P}$ = 10.7 Hz), 133.1, 134.2, 138.3, 147.9, 148.3 (d, $J_{C\text{-}P}$ = 4.2 Hz). **^{31}P{^{1}H} NMR** (162 MHz, C_6D_6): δ = 18.26. **^{19}F NMR** (376 MHz, C_6D_6): δ = -76.37. **Mass Spectrum** (+ve ion, EI), *m/z* = 733.3489*. **IR** (Nujol, cm^{-1}): 3065, 2957, 2926, 2866, 1593, 1460, 1376, 1298, 1262, 1174, 1100, 931, 892, 858, 798, 728, 694, 526.

3.4.7. *Synthesis of $L_AGe(=NAr')Cl$ [Ar' = 2,4,6-$Me_3C_6H_2$] (10)*

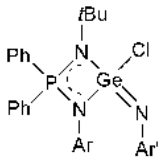

Toluene (20 mL) was added to **L_AGeCl (7)** (0.40 g, 0.75 mmol) using cannula at room temperature. A solution of 2,4,6-$Me_3C_6H_2N_3$ (0.16 mL, 1.00 mmol) in toluene (10 mL) was added drop-wise to the above solution at 0 °C under nitrogen atmosphere. The mixture was stirred for 12 h at room temperature. The volatiles were removed under *vacuo*, then added Et_2O in it and placed for crystallization at 4 °C. The complex was characterized by IR, NMR and Mass spectrometry. Yield: (0.28 g, 58 %). Mp: 210 °C. **^{1}H NMR** (400 MHz, $CDCl_3$): δ = 0.12 (d, $^3J_{H\text{-}H}$ = 6.8 Hz, 6 H, CH*Me$_2$*), 0.99 (d, $^3J_{H\text{-}H}$ = 6.8 Hz, 6 H, CH*Me$_2$*), 1.37 (s, 9 H, *t*Bu), 2.22 (s, 3 H, *p-Me*), 2.54 (s, 6 H, *o-Me*), 3.29 (broad, 2 H, *CH*Me$_2$), 6.84 (s, 2 H, *m-H*), 6.88-6.91 (m, 2 H, Ar), 7.04-7.09 (m, 1 H, Ar), 7.48-7.52 (m, 4 H, Ar), 7.58-7.62 (m, 2 H, Ar), 7.82-7.90 (m, 4 H, Ar). **^{13}C NMR** (100 MHz, $CDCl_3$): δ = 20.3, 20.7, 22.8, 26.0, 28.8, 34.1 (d, $J_{C\text{-}P}$ = 6.6 Hz), 53.9, 124.0, 127.1 (d, $J_{C\text{-}P}$ = 1.9 Hz), 128.1 (d, $J_{C\text{-}P}$ = 26.4 Hz), 128.6 (d, $J_{C\text{-}P}$ = 12.7 Hz), 128.7, 129.0 (d, $J_{C\text{-}P}$ = 6.5 Hz), 129.5, 132.1 (d, $J_{C\text{-}P}$ = 46.5 Hz), 132.8 (d, $J_{C\text{-}P}$ = 2.4 Hz), 133.9 (broad), 140.1, 149.6 (d, $J_{C\text{-}P}$ = 3.2 Hz). **^{31}P{^{1}H} NMR** (162 MHz, $CDCl_3$): δ = 30.49. **Mass Spectrum** (+ve ion, EI), *m/z* = 566.2852 [M-(C_9H_2NCl)]$^+$. **IR** (Nujol, cm^{-1}): 2953, 2923, 2855, 1659, 1632, 1460, 1375, 1319, 1297, 1245, 1196, 1130, 1109, 981, 897, 856, 797, 746, 723, 698.

* = the compound decomposed to ligand.

5. Summary

In this thesis the ligands $\mathbf{L_A}$ and $\mathbf{L_B}$ were used as backbone in stabilizing the low valent tin complexes. The lithium salt $\mathbf{L_A}Li\cdot 2OEt_2$ was prepared *insitu* by deprotonating the ligand by using *n*BuLi and it is used as a good precursor for stabilizing low valent group 14 metal complexes. The reaction of $\mathbf{L_A}$SnCl with KO*t*Bu and $LiN(SiMe_3)_2$ to form the corresponding tin alkoxide and amide products respectively. The iminophoshponamide ligand supported tin complexes were prepared $(\mathbf{L_A})_2$Sn **(2)**, $\mathbf{L_A}$SnO*t*Bu **(3)**, $\mathbf{L_A}SnN(SiMe_3)_2$ **(4)**. When the $\mathbf{L_A}$SnCl **(1)** was reacted with $Li[Al(OCH(CF_3)_2)_4]$ to form cationic tin complex $[\mathbf{L_A}Sn]^+[Al(OCH(CF_3)_2)_4]^-$ **(5)** and its conversion to neutral three coordinated tin complex $\mathbf{L_A}SnOCH(CF_3)_2$ **(6)**.

The *bis*(phosphinimino)amide ligand stabilized chlorostannylene complex acts as a good precursor to study the reactivity studies around metal centre. The $\mathbf{L_B}$SnCl **(7)** was prepared and characterized structurally which adopts three coordinated metal centre forms distorted tetrahedral environments in which the lone pair of electrons occupying one of the vertexes. The reaction of $\mathbf{L_B}$SnCl **(7)** with weakly coordinated $Li[Al(OCH(CF_3)_2)_4]$ complex yielded the tin cationic species $[\mathbf{L_B}Sn]^+[Al(OCH(CF_3)_2)_4]^-$ **(8)**. Oxidation of $\mathbf{L_A}$GeCl with Organic azides (2,4,6-$Me_3C_6H_2N_3$) to form the expected product $\mathbf{L_A}$Ge(=NAr')Cl (Ar' = 2,4,6-$Me_3C_6H_2$) **(10)**.

6. Future directions

The work described in this thesis by using the newly designed which can provide kinetic stabilization for various metal complexes. The synthesis of mono anionic chlorostannylene complex acts as a good precursor for studying the reactivity studies around metal centre and also oxidation of metal. The cationic complexes are useful in studying polymerization and also activation of small molecules.

Crystal Data and Refinement Details

Table 1. Crystal data and structure refinement details for $(L_A)_2Sn$ (2).

Empirical formula	$0.5(C_{56}H_{70}N_4P_2Sn)$
Formula weight	489.93
Temperature	100.0(2) K
Wavelength	0.71073 Å
Crystal system	Monoclinic
Space group	$P2_1/c$
Unit cell dimensions	a = 13.587(3) Å
	b = 18.082(4) Å β = 105.26(3)°
	c = 22.056(1) Å
Volume	5227.4(1) Å
Z	8
Density (calculated)	1.245 Mg/m^3
Absorption coefficient	0.589 (MoKα)/mm^{-1}
F(000)	2055
Crystal size	0.19 x 0.21 x 0.18 mm^3
2θ range for data collection	6.00 to 55.00°
Index ranges	$-16 \le h \le 16, -21 \le k \le 21, -26 \le l \le 26$
Reflections collected	46524
Independent reflections	9570 (R_{int} = 0.0564)
Completeness to θ = 58.99°	99.0%
Refinement method	Full-matrix least-squares on F^2
Data/ restrains/ parameters	9570 / 0 / 756
Goodness-of-fit on F^2	1.044
Final R indices (I>2 σ(I))	R1 = 0.0382, wR2 = 0.0891
R indices (all data)	R1 = 0.0444, wR2 = 0.0950
Largest diff. Peak and hole	1.116 and -0.618 e.$Å^{-3}$
Diffractometer & detector	Rigaku XtaLAB mini diffractometer & Mercury375M CCD detector
Detector distance & tube power	49.85mm & (50KV, 12mA).

Table 2. Crystal data and structure refinement details for L_ASnO*t*Bu (3).

Empirical formula	$C_{35}H_{45}N_2PSnO$
Formula weight	623.36
Temperature	100.0(2) K
Wavelength	0.71073 Å
Crystal system	Monoclinic
Space group	$P2_1/n$
Unit cell dimensions	a = 9.087(4) Å
	b = 21.525(4) Å β = 94.67(3)°
	c = 15.884(3) Å
Volume	3096.5(1) Å
Z	4
Density (calculated)	1.340 Mg/m^3
Absorption coefficient	0.903 (MoKα)/mm^{-1}
F(000)	1296
Crystal size	0.18 x 0.19 x 0.21 mm^3
2θ range for data collection	5.68 to 64.34°
Index ranges	$-10 \le h \le 10$, $-26 \le k \le 26$, $-18 \le l \le 18$
Reflections collected	56288
Independent reflections	5657 (R_{int} = 0.0289)
Completeness to θ = 58.99°	100.%
Refinement method	Full-matrix least-squares on F^2
Data/ restrains/ parameters	5657 / 0 / 344
Goodness-of-fit on F^2	1.061
Final R indices (I>2 σ(I))	R1 = 0.0221, wR2 = 0.0568
R indices (all data)	R1 = 0.0244, wR2 = 0.0584
Largest diff. Peak and hole	0.058 and -0.335 e.$Å^{-3}$
Diffractometer detector	Bruker *AXS* KAPPA APEX-II CCD diffractometer
Detector distance, tube power	50mm & (50KV, 30mA)

Table 3. Crystal data and structure refinement details for $L_ASnOCH(CF_3)_2$ (6).

Empirical formula	$C_{31}H_{37}N_2PSnO$
Formula weight	717.33
Temperature	100.0(2) K
Wavelength	0.71073 Å
Crystal system	Monoclinic
Space group	$P2_1/n$
Unit cell dimensions	a = 9.547(2) Å
	b = 21.766(1) Å β = 95.375(3)°
	c = 15.316(2) Å
Volume	3168.7(1) Å
Z	4
Density (calculated)	1.504 Mg/m^3
Absorption coefficient	0.919 (MoKα)/mm^{-1}
F(000)	1455
Crystal size	0.22 x 0.19 x 0.20 mm^3
2θ range for data collection	6.00 to 55.00°
Index ranges	$-11 \le h \le 11$, $-26 \le k \le 14$, $-18 \le l \le 9$
Reflections collected	9417
Independent reflections	5720 (R_{int} = 0.0414)
Completeness to θ = 58.99°	100%
Refinement method	Full-matrix least-squares on F^2
Data/ restrains/ parameters	5720 / 0 / 385
Goodness-of-fit on F^2	1.055
Final R indices (I>2 σ(I))	R1 = 0.0343, wR2 = 0.0831
R indices (all data)	R1 = 0.0377, wR2 = 0.0873
Largest diff. Peak and hole	0.659 and -0.704 e.$Å^{-3}$
Diffractometer detector	Rigaku XtaLAB mini diffractometer & Mercury375M CCD detector
Detector distance, tube power	49.85mm & (50KV, 12mA).

Table 4. Crystal data and structure refinement details for L_BSnCl (7).

Empirical formula	$C_{48}H_{54}ClN_3P_2Sn\ 0.5(C_2H_5O)$	
Formula weight	923.11	
Temperature	100.0(2) K	
Wavelength	0.71073 Å	
Crystal system	Triclinic	
Space group	$P\bar{1}$	
Unit cell dimensions	a = 12.149(3) Å	α = 69.174(2)°
	b = 13.015(2) Å	β = 82.470(3)°
	c = 22.056(1) Å	γ = 77.40(2)°
Volume	2284.4(2) Å	
Z	2	
Density (calculated)	1.341 Mg/m^3	
Absorption coefficient	0.726 (MoKα)/mm^{-1}	
F(000)	955	
Crystal size	0.22 x 0.18 x 0.19 mm^3	
2θ range for data collection	6.4 to 55.00°	
Index ranges	$-14 \le h \le 14, -15 \le k \le 15, -19 \le l \le 19$	
Reflections collected	20567	
Independent reflections	8326 (R_{int} = 0.0337)	
Completeness to θ = 58.99°	100%	
Refinement method	Full-matrix least-squares on F^2	
Data/ restrains/ parameters	8326 / 0 / 529	
Goodness-of-fit on F^2	1.034	
Final R indices (I>2 σ(I))	R1 = 0.0345, wR2 = 0.0907	
R indices (all data)	R1 = 0.0363, wR2 = 0.0890	
Largest diff. Peak and hole	1.822 and -2.161 e.$Å^{-3}$	
Diffractometer detector	Rigaku XtaLAB mini diffractometer & Mercury375M CCD detector	
Detector distance, tube power	49.85mm & (50KV, 12mA).	

7. References:

1) Asay, M.; Jones, C.; Driess, M. *Chem. Rev.* **2011,** *111*, 354.
2) Nagendran, S.; Roesky, H. W. *Organometallics* **2008**, *27*, 457.
3) Mandal, S. K.; Roesky, H. W. *Chem. Commun.* **2010**, *46*, 6016.
4) Barrau, J.; Rima, G. *Coord. Chem. Rev.* **1998**, *178−180*, 593.
5) Mizuhata, Y.; Sasamori, T.; Tokitoh, N. *Chem. Rev.* **2009**, *109*, 3479.
6) Bourissou, D.; Guerret, O.; Gabbai, F. P.; Bertrand, G. *Chem. Rev.* **2000**, *100*, 39.
7) Liddle, S. T.; Edworthy, I. S.; Arnold, P. L. *Chem. Soc. Rev.* **2007**, *36*, 1732.
8) Cantat, T.; Mezailles, N.; Auffrant, A.; Le Floch, P. *Dalton Trans.* **2008**, 1957.
9) Hahn, F. E. *Angew. Chem., Int. Ed.* **2006**, *45*, 1348.
10) Hahn, F. E.; Jahnke, M. C. *Angew. Chem., Int. Ed.* **2008**, *47*, 3122.
11) Kaufhold, O.; Hahn, E. E. *Angew. Chem., Int. Ed.* **2008**, *47*, 4057.
12) Greenwood and Earnshaw, *Chemistry of the elements.*2nd edition.
13) Gonzalez S. D. *N-Heterocyclic Carbenes.*
14) P. Jutzi, H. J. Hoffmann, D. J. Brauer, C. Krüger, *Angew. Chem.* **1973**, *85*, 1116; (b) J. Satgé, M. Massol, P. Rivière, *J. Organomet. Chem.* **1973**, *56*, 1.
15) (a) Edelmann, F. T. *Coord. Chem. Rev.* **1994**, *137*, 403; (b) Barker, J.; Kilner, M. *Coord. Chem. Rev.* **1994**, *133*, 219; (c) Edelmann, F. T. *Chem. Soc. Rev.* **2009**, *38*, 2253; (d) Edelmann, F. T. *Chem. Soc. Rev.* **2012**, *41*, 7657.
16) Steiner, A.; Zacchini, S.; Richards, P. I. *Coord. Chem. Rev.* **2002,** *227,* 193.
17) Baier, F.; Fei, Zhaofu.; Gornitzka, H.; Murso, A.; Neufeld, S.; Pfeiffer, M.; Rüdenauer, I.; Steiner, A.; Stey, T.; Stalke, D. *J. Organomet. Chem.* **2002,** *661,* 111.
18) Witt, M.; Roesky, H. W. *Chem. Rev.* **1994,** *94,* 1163.
19) Neumann, W. P. *Chem. Rev.* **1991**, *91*, 311.
20) Bigwood, M. P.; Corvan, P. J.; Zuckerman, J. J. *J. Am. Chem. Soc.* **1981**, *103*, 7643.
21) West, R. *Science*, **1984**, *225*, 1109.
22) Harris, D. H.; Lappert, M.F.; Pedley, J. B.; Sharp, G. J. *J. Chem. Soc., Dalton Trans.* **1976**, *11*, 945.
23) Dehnicke, K.; Ergezinger, C.; Hartmann, E.; Zinn, A. *J. Organomet. Chem.* **1988,** *352*, C1.
24) Nimitsiriwat, N.; Gibson, V. C.; Marshall, E. L.; White, A. J. P.; Dale, S. H.; Elsegood, M. R. J. *Dalton Trans.* **2007,** 4464.
25) Sen, S. S.; Kritzler-Kosch, M. P.; Nagendran, S.; Roesky, H. W.; Beck, T.; Pal, A.;

Herbst-Irmer, R. *Eur. J. Inorg. Chem.* **2010,** 5304.

26) Olah, G. A. *J. Am. Chem. Soc.* **1972**, *94*, 808.

27) Schäfer, A.; Winter, F.; Saak, W.; Haase, D.; Pöttgen, R.; Müller, T. *Chem. – Eur. J.* **2011**, *17*, 10979.

28) Swamy, V. S. V. S. N.; Pal, S.; Khan, S.; Sen, S. S. Dalton Trans. **2015**, *44*, 12903.

29) Jutzi, P.; Kohl, F.; Hofmann, P.; Krüger, C.; Tsay, Y. *Chem. Ber.* **1980**, *113*, 757.

30) Probst, T.; Steigelmann, O.; Riede, J.; Schmidbaur, H. *Angew. Chem., Int. Ed. Engl.* **1990**, *29*, 1397.

31) Schmidbaur, H.; Schier, A. *Organometallics*, **2008**, *27*, 2361.

32) (a) Lambert, J. B.; *Science*, **2008**, *322*, 1333; (b) Müller, T.; *Angew. Chem., Int. Ed.* **2009**, *48*, 3740.

33) Singh, A. P.; Roesky, H. W.; Carl, E.; Stalke, D.; Demers, J.-P.; Lange, A. *J. Am. Chem. Soc.* **2012**, *134*, 4998.

34) Bouska, M.; Dostal, L.; Ruzicka, A.; Jambor, R. *Organometallics* **2013**, *32*, 1995.

35) Taylor, M. J.; Saunders, A. J.; Coles, M. P.; Fulton, J. R. *Organometallics* **2011**, *30*, 1334.

36) (a) Inés, B.; Patil, M.; Carreras, J.; Goddard, R.; Thiel, W.; Alcarazo, M. *Angew. Chem., Int. Ed.* **2011**, *50*, 8400; (b) Khan, S.; Gopakumar, G.; Thiel, W.; Alcarazo, M. *Angew. Chem., Int. Ed.* **2013**, *52*, 5644.

37) (a) Dias, H. V. R.; Jin, W. *Inorg. Chem.* **1996**, *35*, 6546. (b) Ayers, A. E.; Marynick, D. S.; Dias, H. V. R. *Inorg. Chem.* **2000**, *39*, 4147.

38) (a) Ding, Y.; Roesky, H. W.; Noltemeyer, M.; Schmidt, H. G. *Organometallics* **2001**, *20*, 1190; (b) Ding, Y.; Roesky, H. W.; Noltemeyer, M.; Schmidt, H.G. *Organometallics* **2001**, *20*, 4806.

39) Aubrecht K. B.; Hillmyer M. A.; Tolman W. B. *Macromolecules.* **2002**, *35*, 644-650.

40) Aubrecht, K. B.; Hillmyer, M. A.; Tolman, W. B. *Macromolecules* **2002**, *35*, 644.

41) Dolomanov, O. V.; Bourhis, L. J.; Gildea, R. J.; Howard, J. A. K.; Puschmann, H.; *J. Appl. Crystallogr.* **2009**, *42*, 339.

42) Sheldrick, G. M. *Acta Crystallogr. Sect. A.* **2008**, *64*, 112.

43) CrystalClear 2.0, Rigaku Corporation, Tokyo, Japan.

44) Murata, S.; Abe, S.; Tomioka, H. *Journal of Organic chemistry.* **1997**, *62*, 3055-3061.

45) Prashanth, B.; Singh, S. *Unpublished results*

46) Prashanth, B.; Singh, S. *Dalton Trans.***2016**, *45*, 6079-6087.

47) Ivanova, S. M.; Nolan, B. G.; Kobayashi, Y.; Miller, S. M.; Anderson, O.P.; Strauss, S. H. *Chemistry A European Journal.* **2001**, *7*, No.2, 503-510.

48) Dolomanav, O. V.; Bourhis, L. J.; Gildea, R. J.; Howard, J. A. K.; Puschmann, H. *J. Appl. Cryst.* **2009**, *42*, 339.

49) G. M. Sheldrick, SHELXL-97, Program for Crystal Structure Refinement, Universität Göttingen, Göttingen, FRG, 1997.

50) "SHELXS-97, Program for Structure Solution": G. M. Sheldrick, *Acta Crystallogr., Sect. A,* **2008,** *64*, 112.

51) Spencer, L. P.; Altwer, R.; Wei, D.; Gelmini, L.; Gauld, J.; Stephan, D. W. *Organometallics* **2003,** *22*, 3841.

52) Thapa, I.; Gambarotta, S.; Korobkov, I.; Duchateau, R.; Kulangara, S. V.; Chevalier, R. *Organometallics* **2010,** *29*, 4080.

53) Prashanth, B. PhD. Dissertation, IISER Mohali, 2015.

Supporting Information

Heteronuclear NMR spectra (^{1}H, ^{13}C, ^{31}P and ^{19}F), IR spectra and HRMS spectra of new compounds reported in this dissertion.

Contents

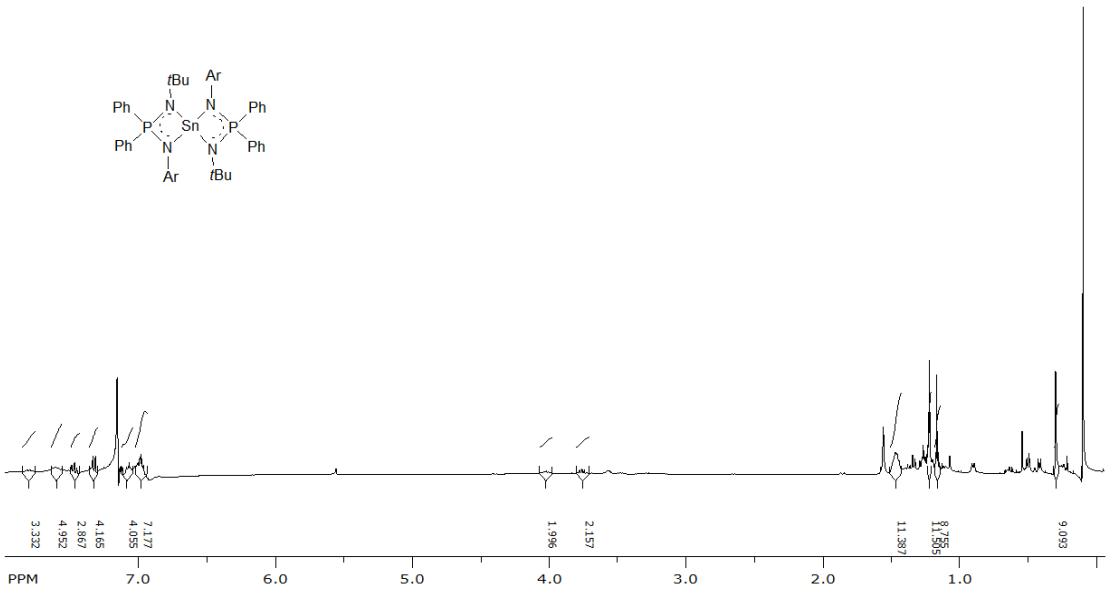

Fig. S1. ^{1}H NMR (400 MHz, C_6D_6) spectrum of $(\mathbf{L_A})_2$Sn (**2**).

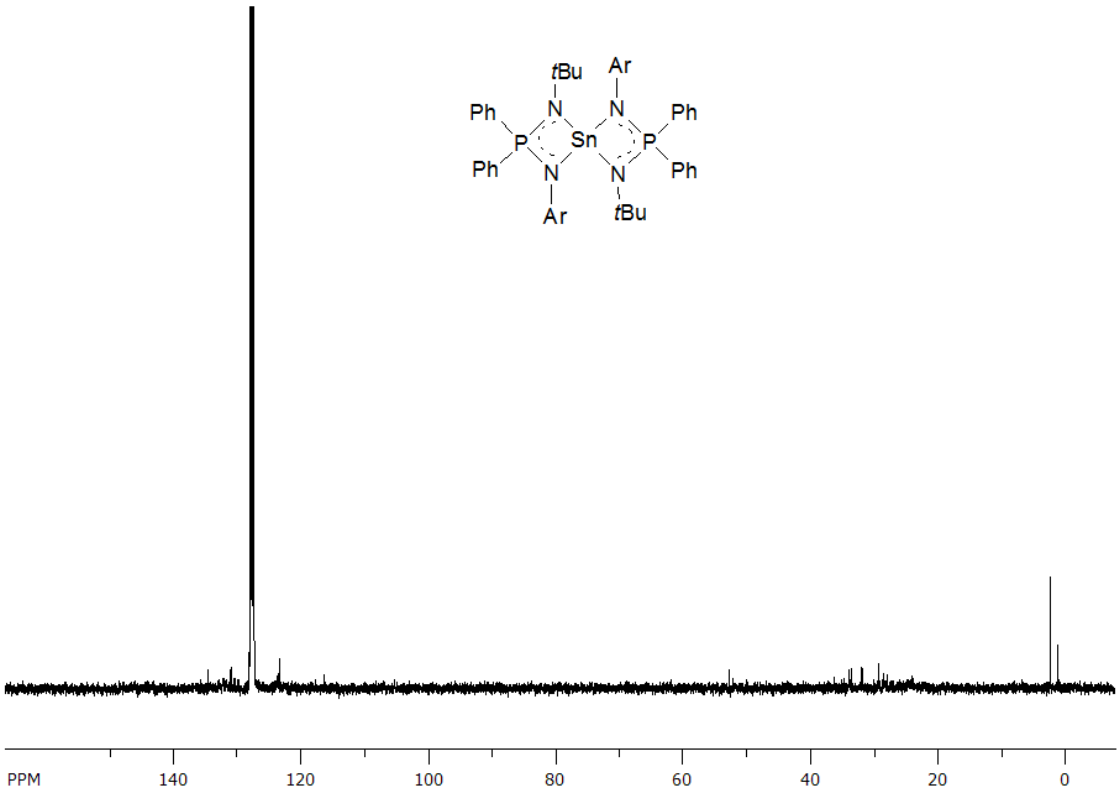

Fig. S2. ^{13}C NMR (100 MHz, C_6D_6) spectrum of $(\mathbf{L_A})_2$Sn (**2**).

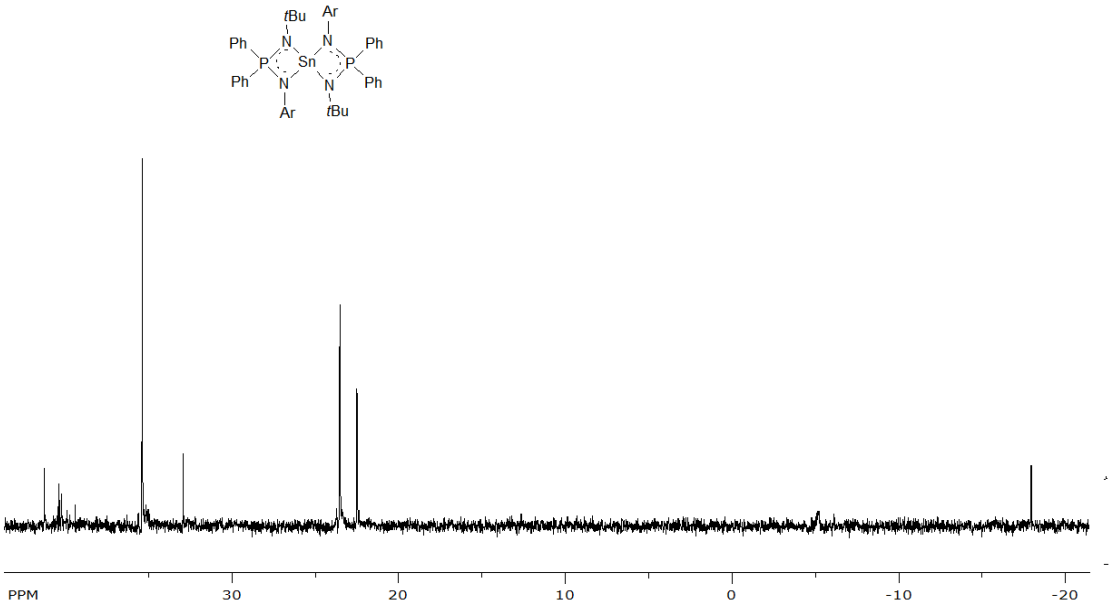

Fig. S3. $^{31}P\{^{1}H\}$ NMR (162 MHz, C_6D_6) spectrum of $(\mathbf{L_A})_2Sn$ **(2)**.

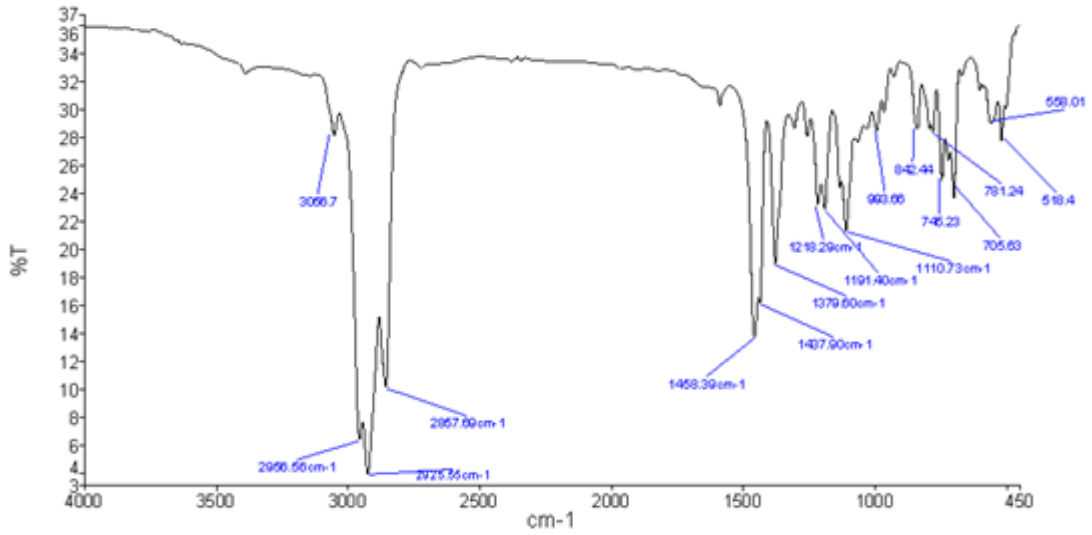

Fig S4. IR spectrum of $(\mathbf{L_A})_2Sn$ **(2)**

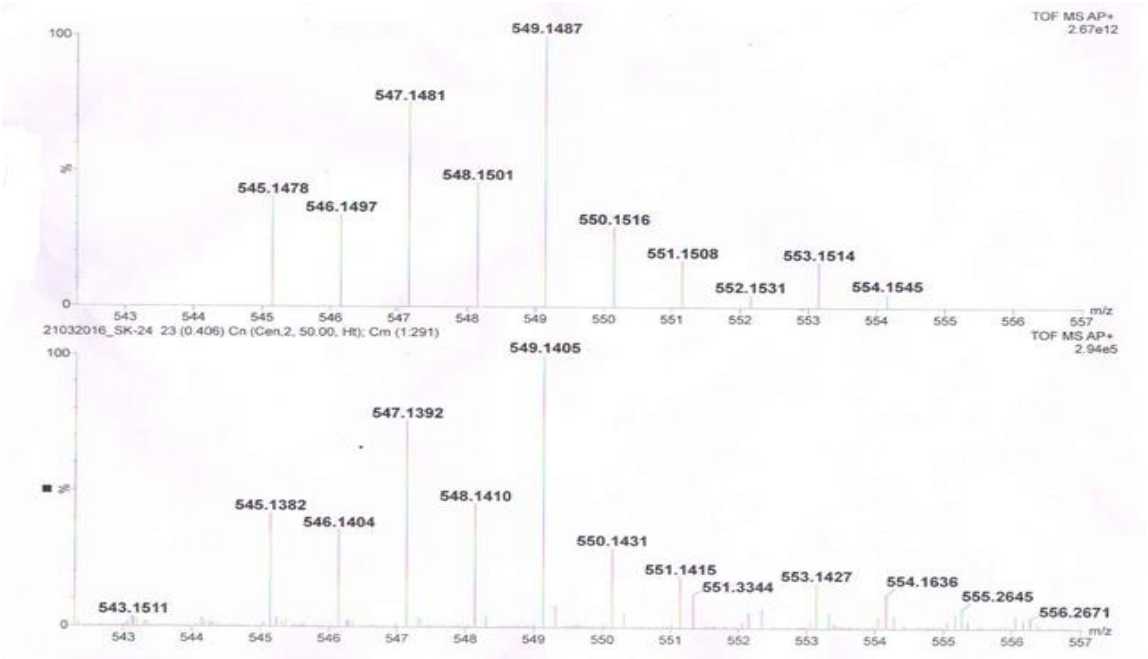

Fig S5. Mass spectrum of $(\mathbf{L_A})_2$Sn **(2)**

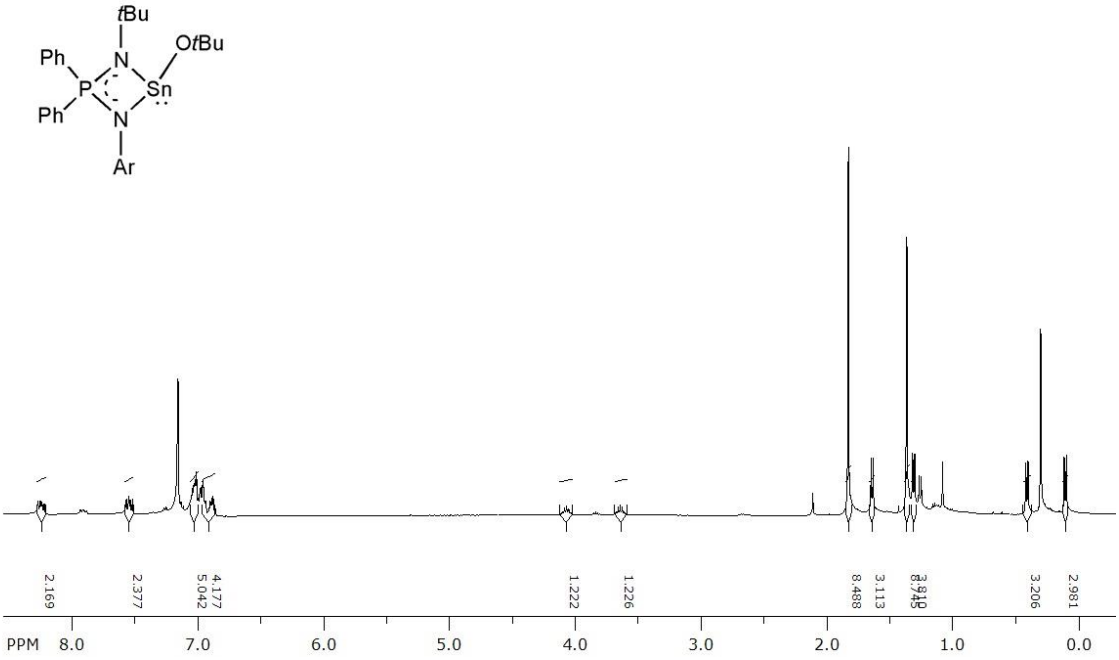

Fig. S6. ^{1}H NMR (400 MHz, C_6D_6) spectrum of $\mathbf{L_A}$Sn*O*t*Bu* (**3**)

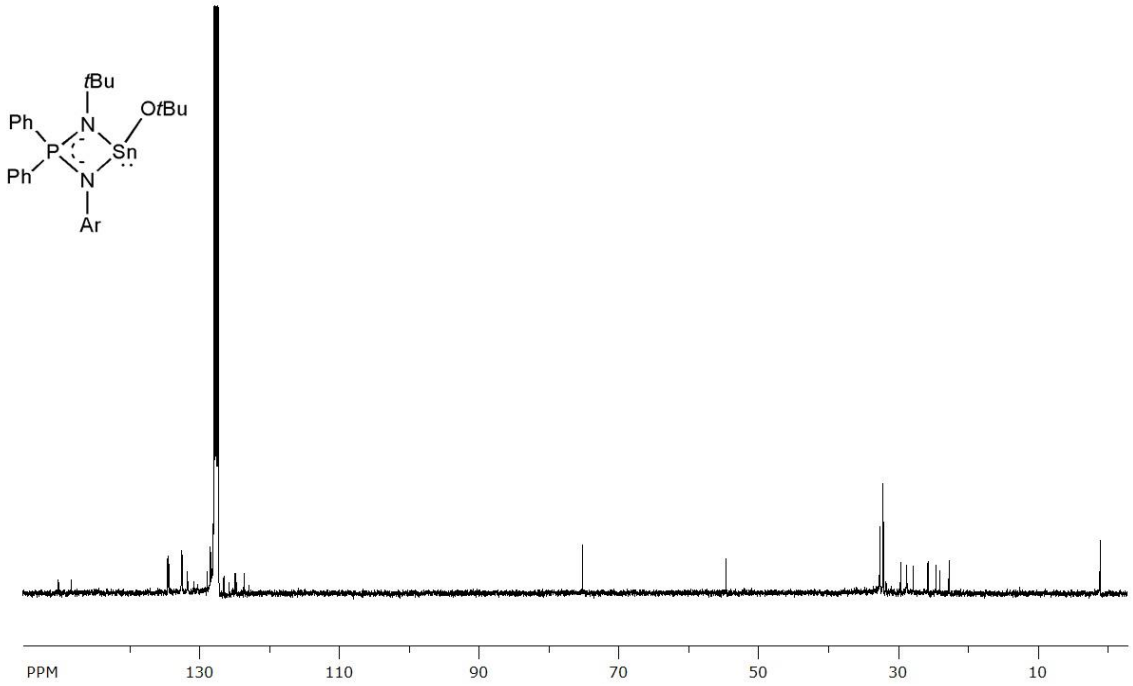

Fig. S7. ^{13}C NMR (100 MHz, C_6D_6) spectrum of $\mathbf{L_A}$SnO*t*Bu **(3)**.

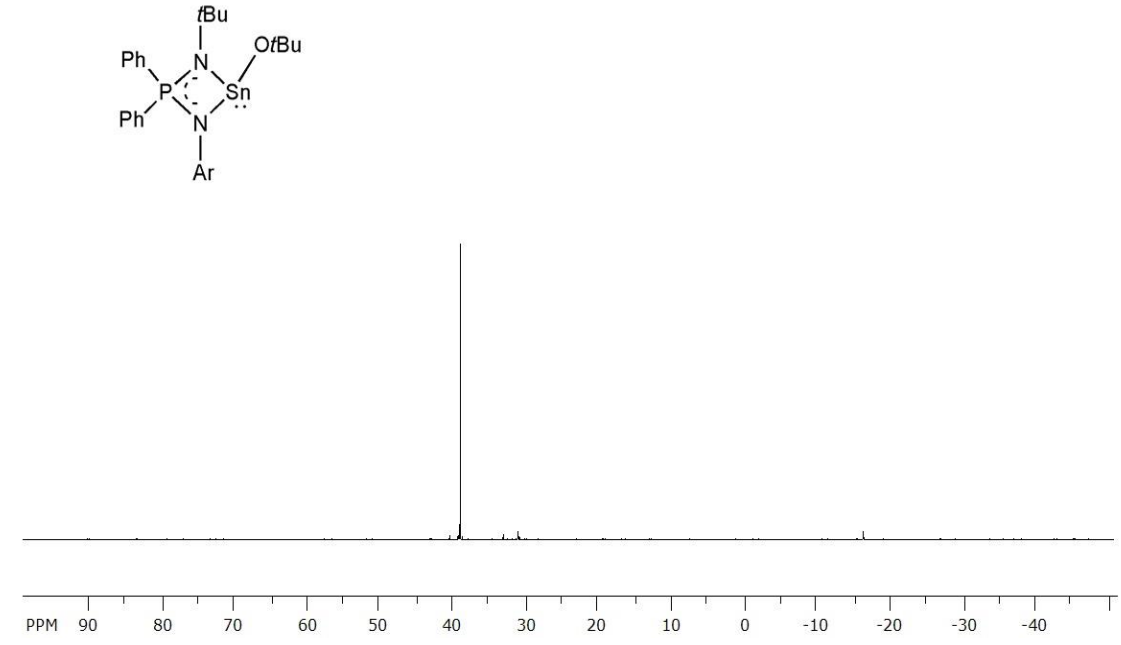

Fig. S8. $^{31}P\{^1H\}$ NMR (162 MHz, C_6D_6) spectrum of $\mathbf{L_A}$SnO*t*Bu **(3)**.

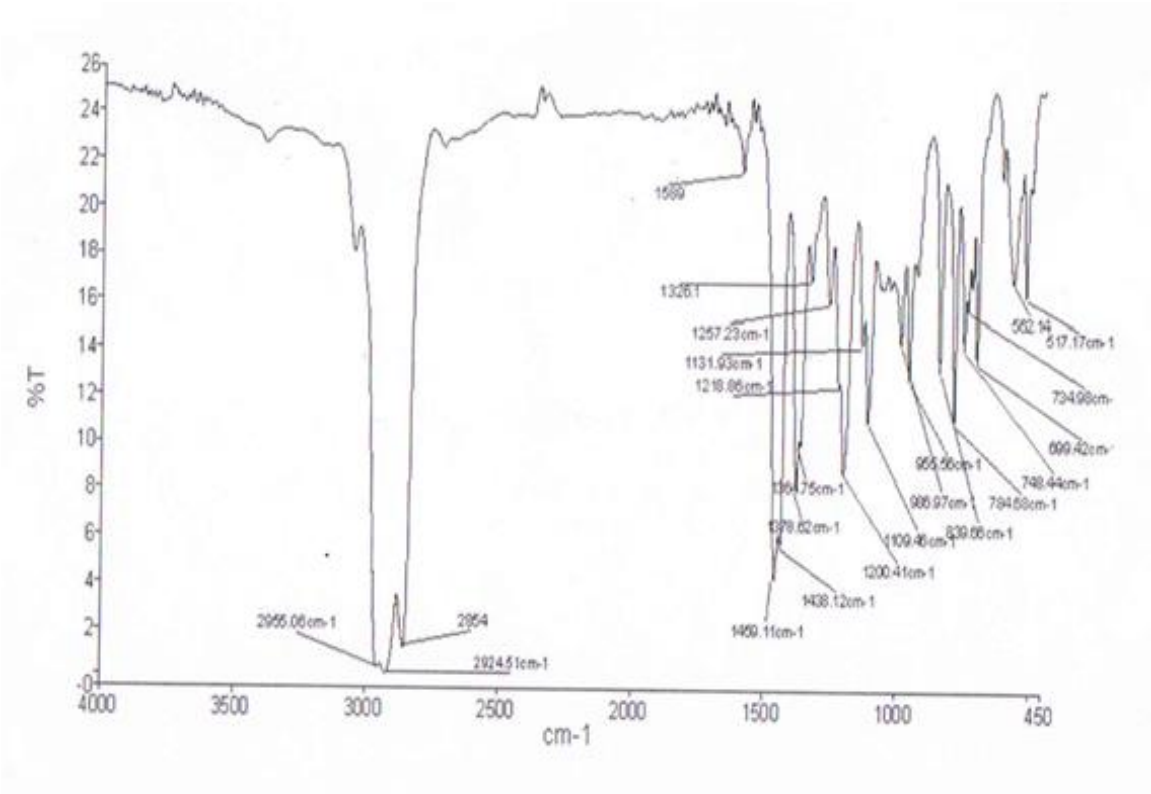

Fig. S9. IR spectrum of $\mathbf{L_A}$SnO*t*Bu **(3)**.

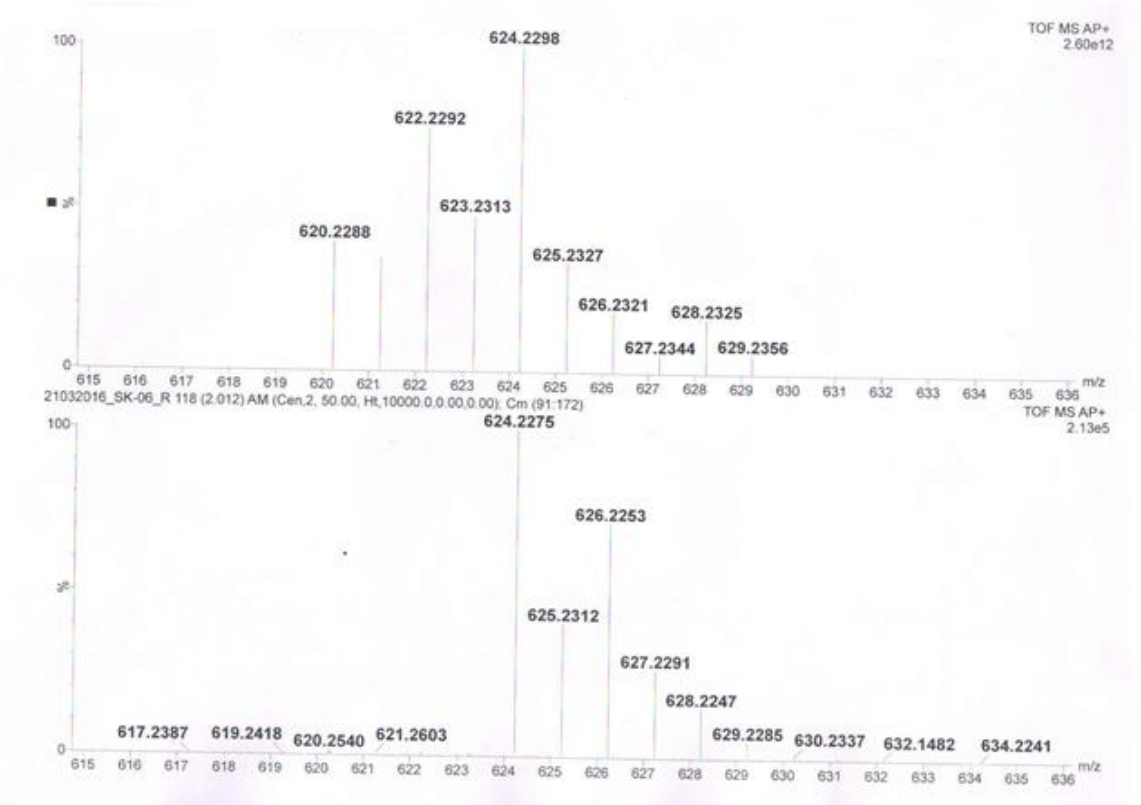

Fig. S10. Mass spectrum of $\mathbf{L_A}$SnO*t*Bu **(3)**.

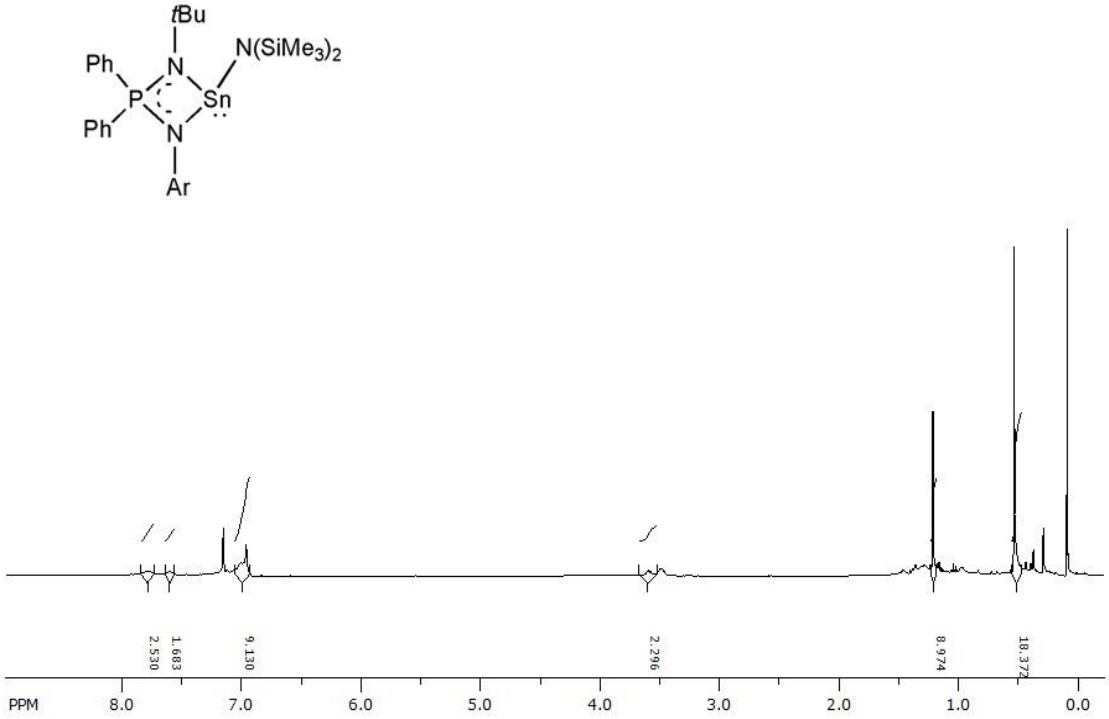

Fig. S11. ^{1}H NMR (400 MHz, C_6D_6) spectrum of $\mathbf{L_A}SnN(SiMe_3)_2$ (**4**)

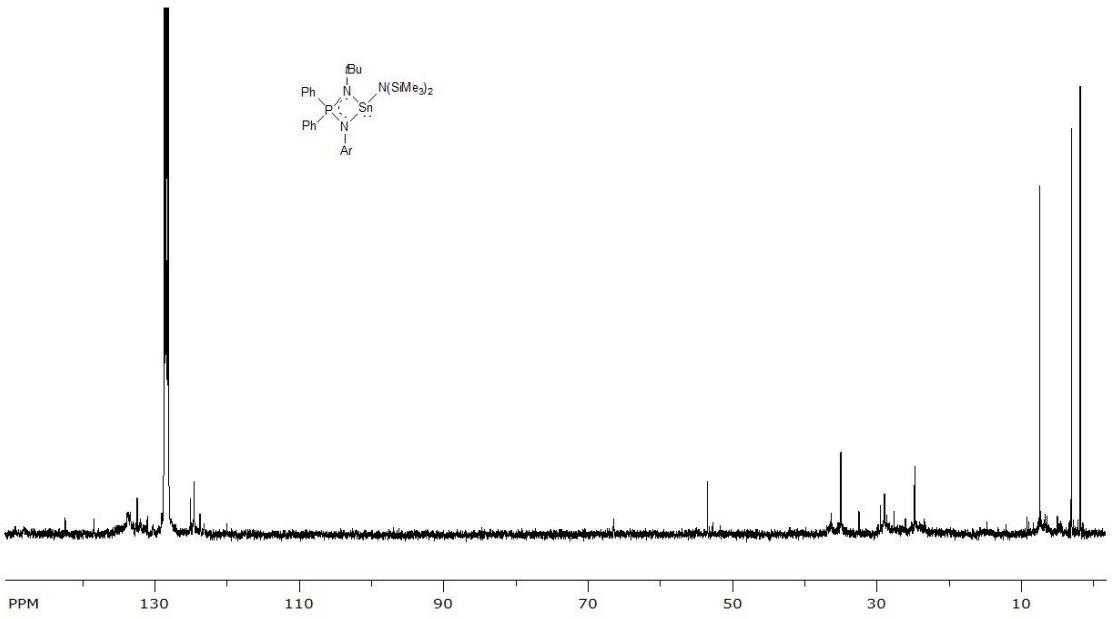

Fig. S12. ^{13}C NMR (100 MHz, C_6D_6) spectrum of $\mathbf{L_A}SnN(SiMe_3)_2$ **(4)**.

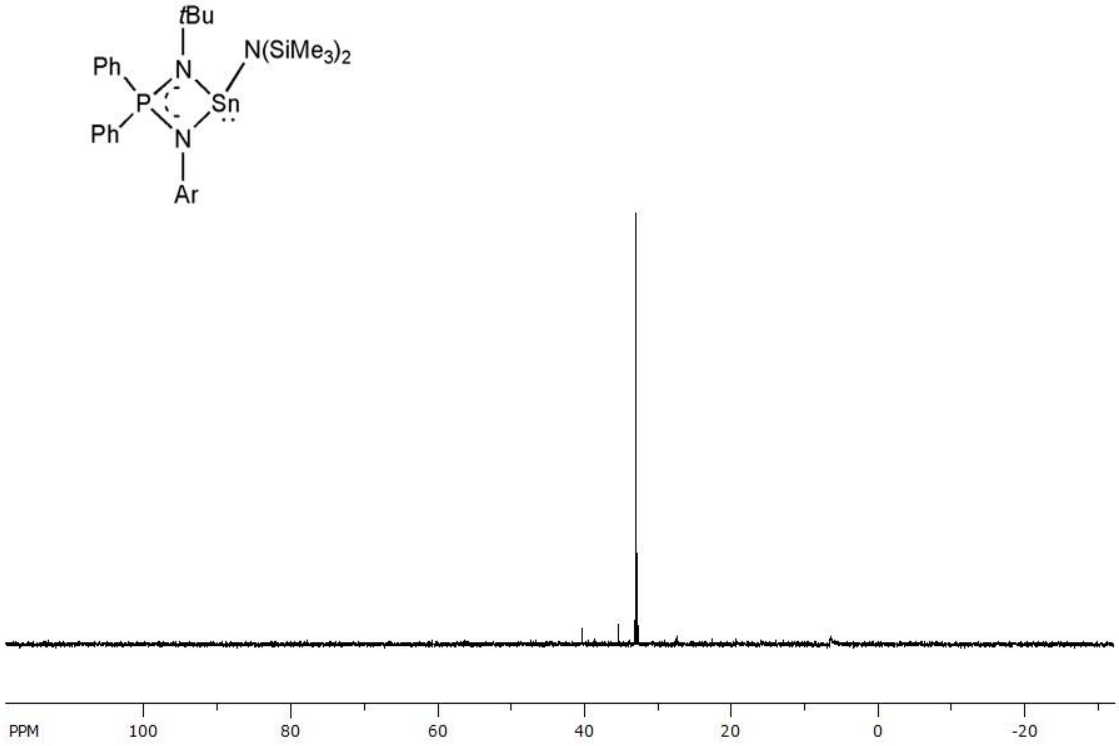

Fig. S13. $^{31}P\{^{1}H\}$ NMR (162 MHz, C_6D_6) spectrum of $\mathbf{L_A}SnN(SiMe_3)_2$ **(4)**

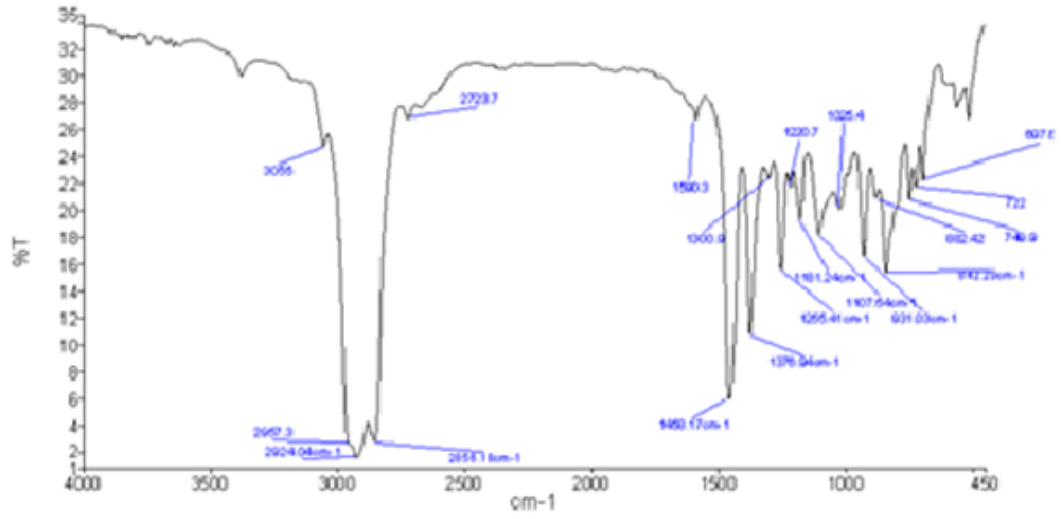

Fig. S14. IR spectrum of $\mathbf{L_A}SnN(SiMe_3)_2$ **(4)**

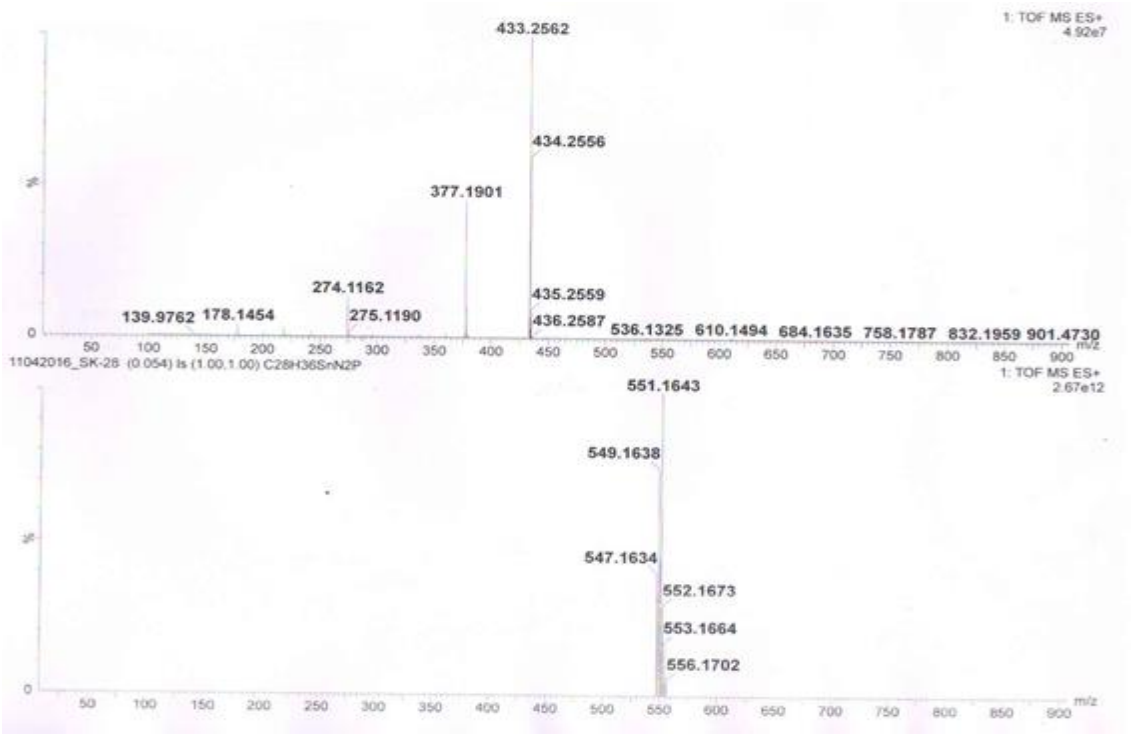

Fig. S15. Mass spectrum of $\mathbf{L_A}SnN(SiMe_3)_2$ **(4)**

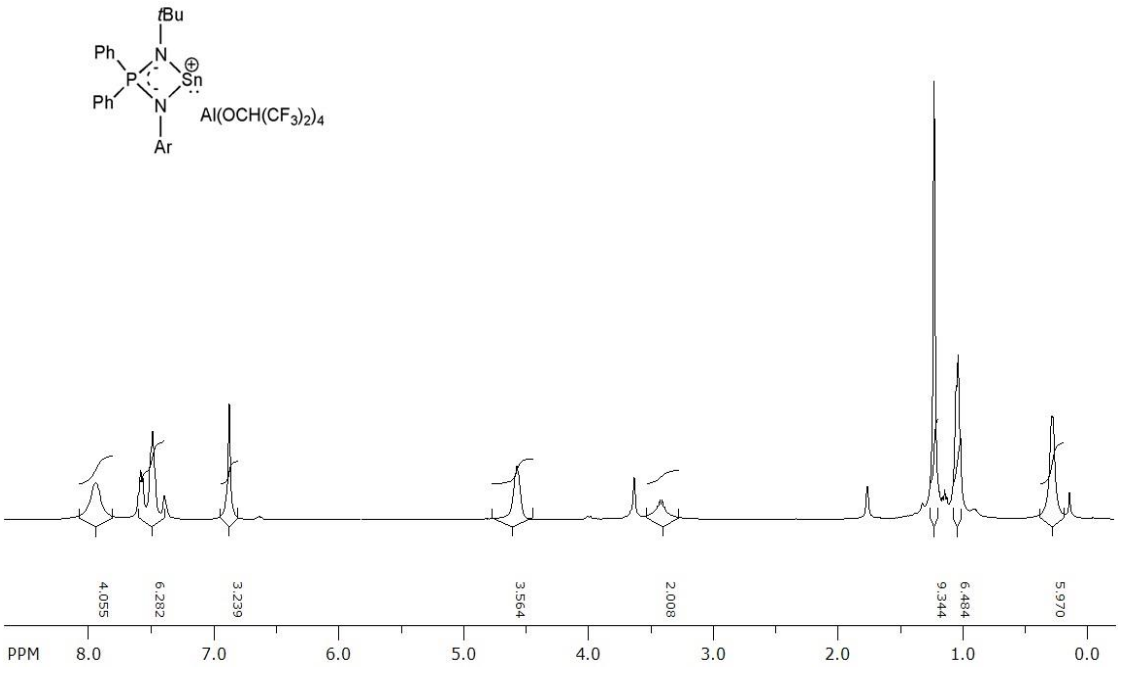

Fig. S16. ^{1}H NMR (400 MHz, THF) spectrum of $[\mathbf{L_A}Sn]^+[Al(OCH(CF_3)_2)_4]^-$ **(5)**.

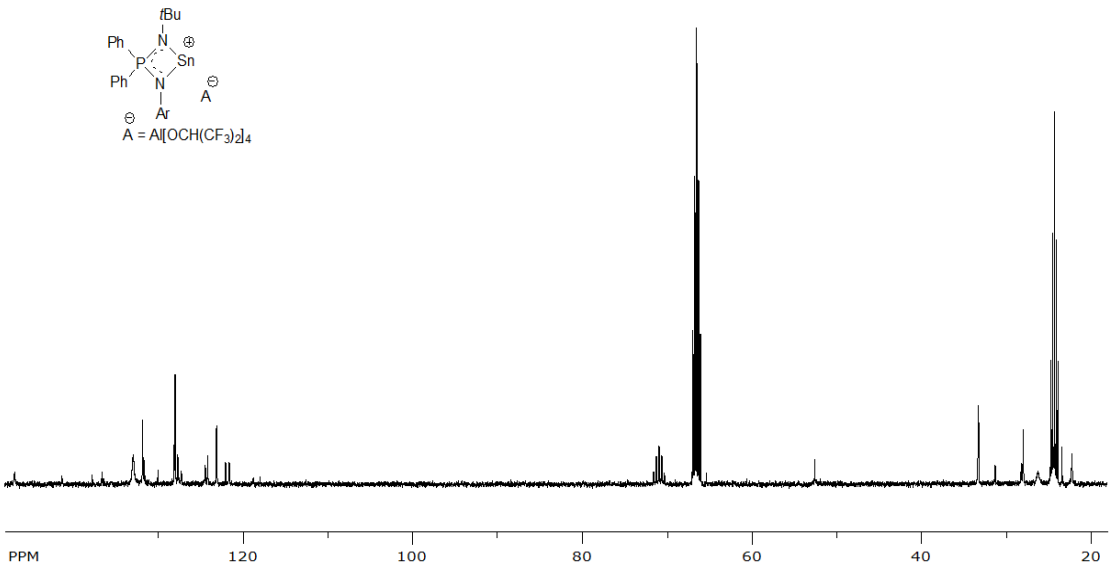

Fig. S17. ^{13}C NMR (100 MHz, THF) spectrum of $[\mathbf{L_A}Sn]^+[Al(OCH(CF_3)_2)_4]^-$ **(5)**

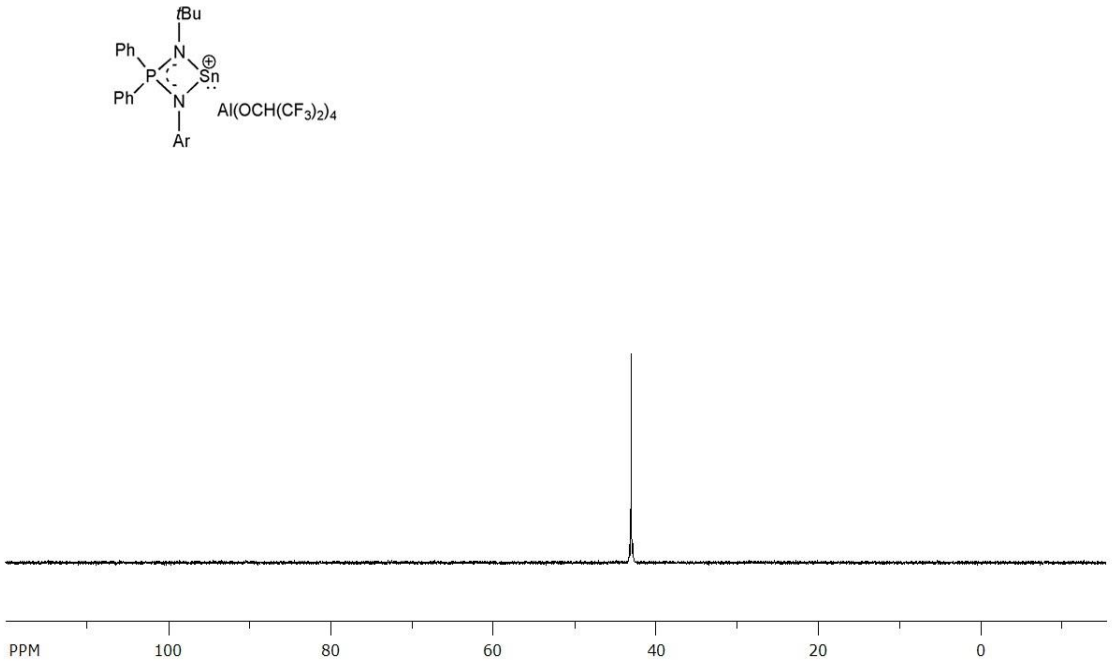

Fig. S18. ^{31}P{^{1}H} NMR (162 MHz, THF) spectrum of $[\mathbf{L_A}Sn]^+[Al(OCH(CF_3)_2)_4]^-$ **(5)**

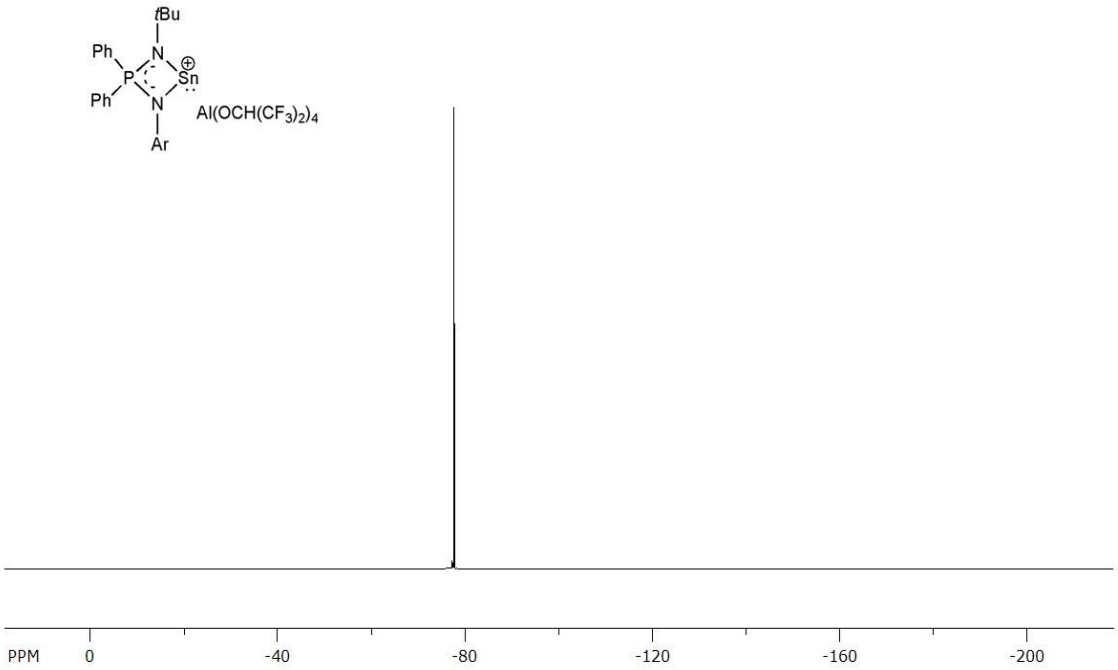

Fig. S19. ^{19}F NMR (376 MHz, THF) spectrum of $[\mathbf{L_A}Sn]^+[Al(OCH(CF_3)_2)_4]^-$ **(5)**.

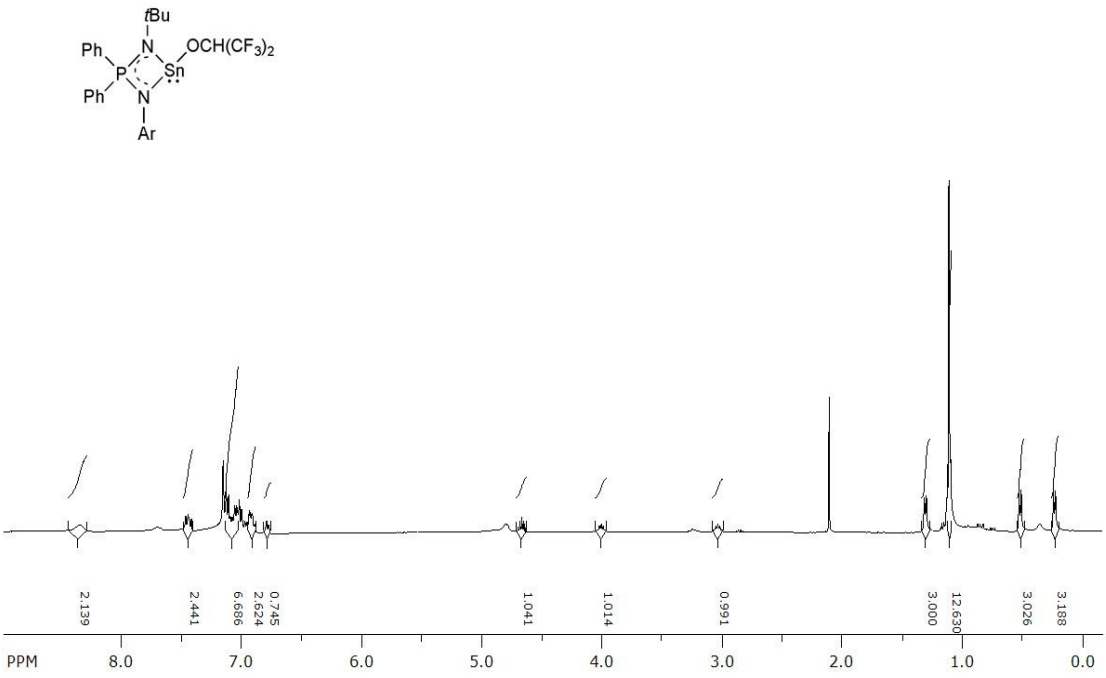

Fig. S20. ^{1}H NMR (400 MHz, C_6D_6) spectrum of $\mathbf{L_A}SnOCH(CF_3)_2$ **(6)**.

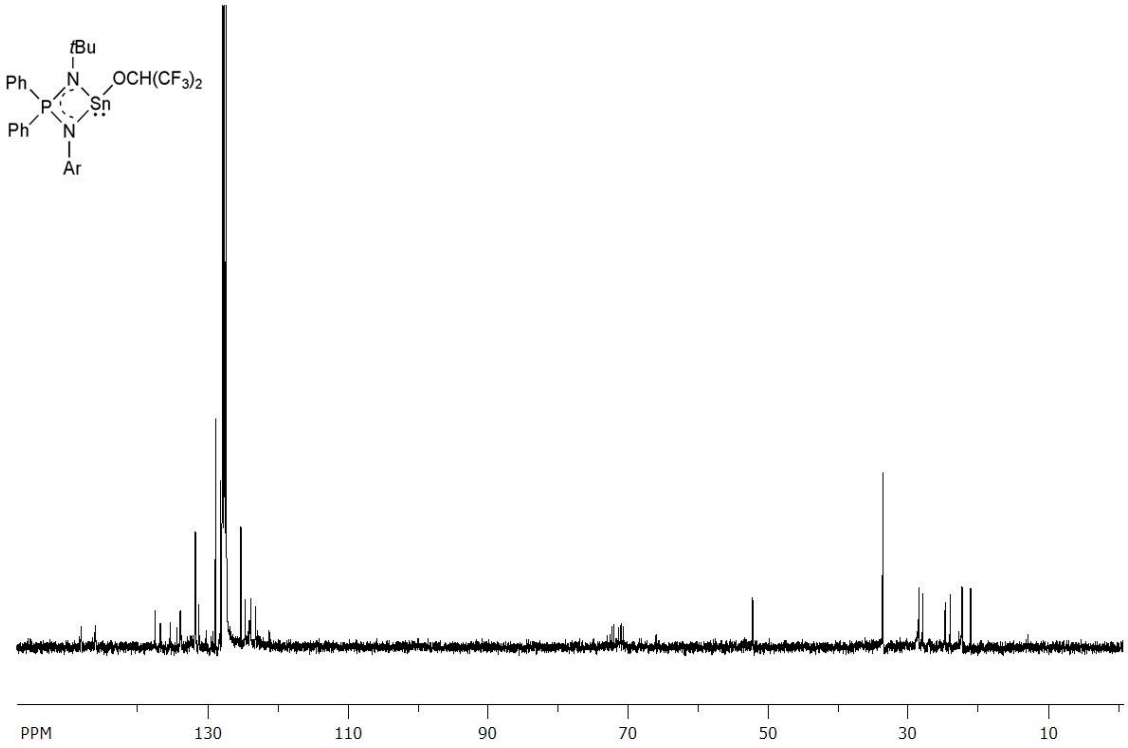

Fig. S21. ^{13}C NMR (100 MHz, C_6D_6) spectrum of $\mathbf{L_A}SnOCH(CF_3)_2$ **(6)**.

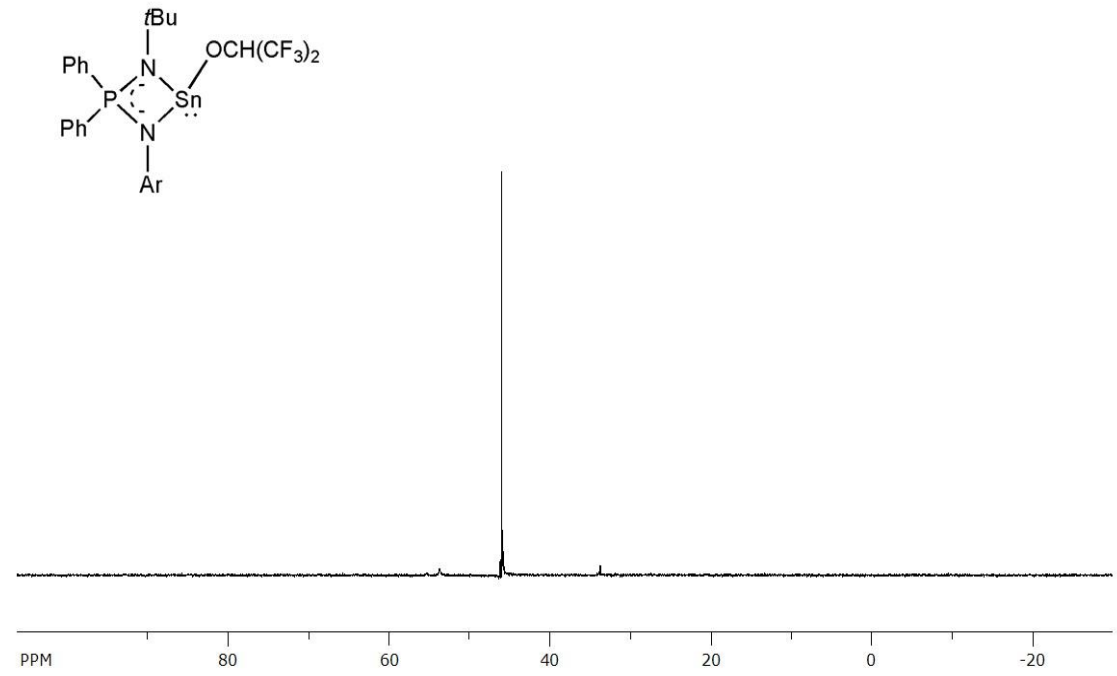

Fig. S22. $^{31}P\{^1H\}$ NMR (162 MHz, C_6D_6) spectrum of $\mathbf{L_A}SnOCH(CF_3)_2$ **(6)**

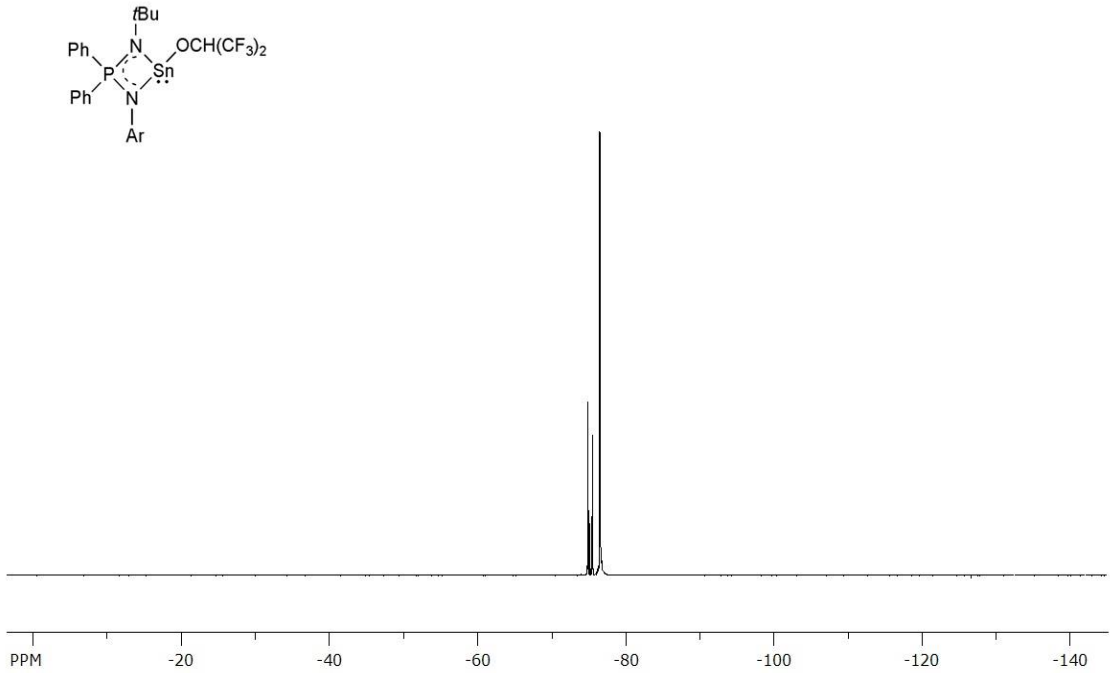

Fig. S23. ^{19}F NMR (376 MHz, C_6D_6) spectrum of $\mathbf{L_A}SnOCH(CF_3)_2$ **(6)**.

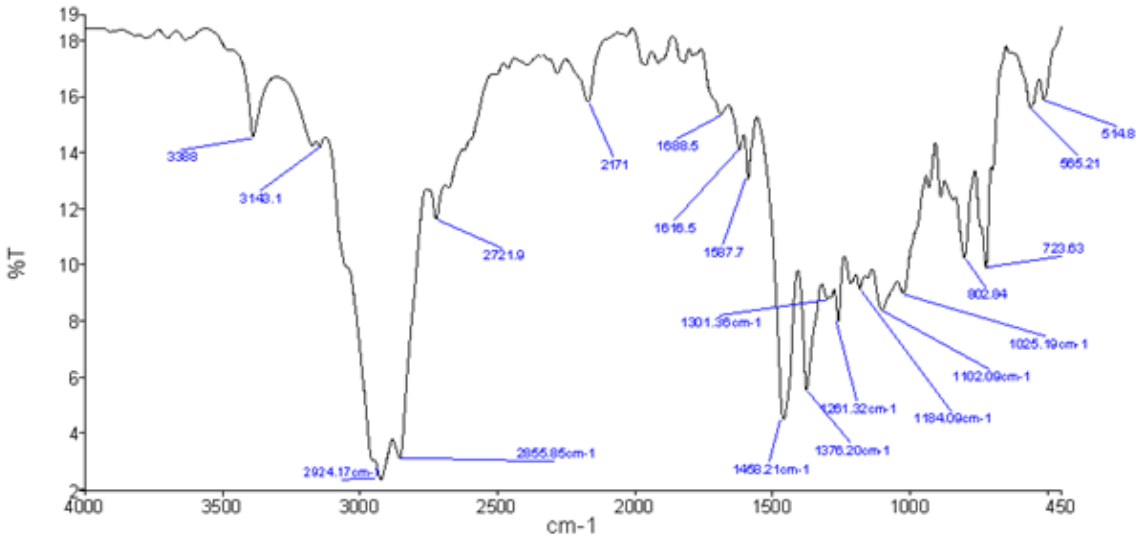

Fig. S24. IR spectrum of $\mathbf{L_A}SnOCH(CF_3)_2$ **(6)**.

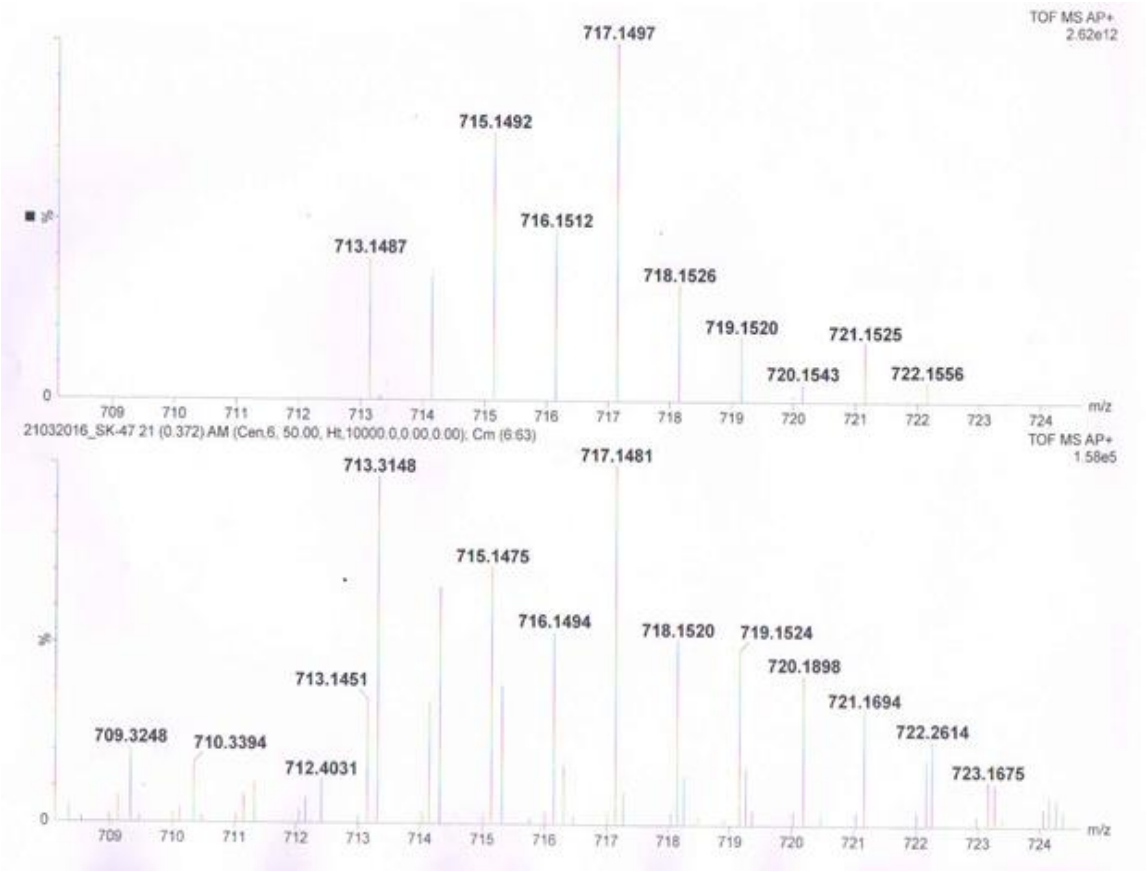

Fig. S25. Mass spectrum of $\mathbf{L_A}SnOCH(CF_3)_2$ **(6)**.

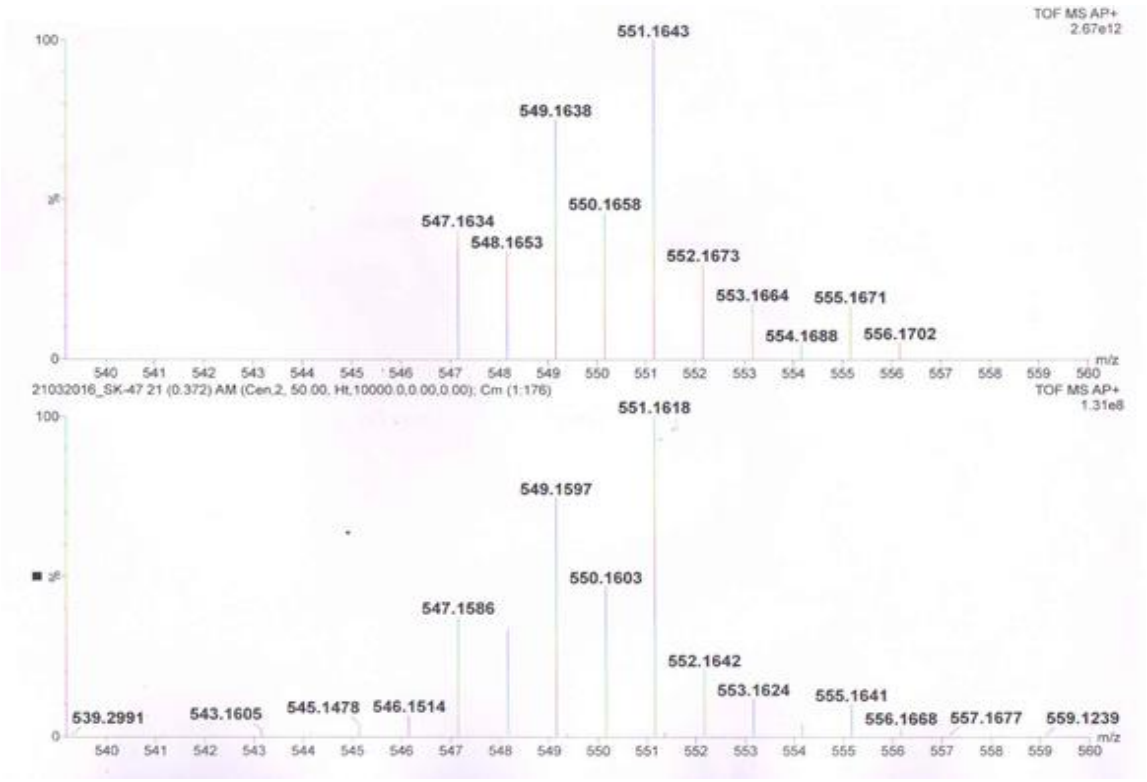

Fig. S26. Mass spectrum of $\mathbf{L_A}SnOCH(CF_3)_2$ **(6)**.

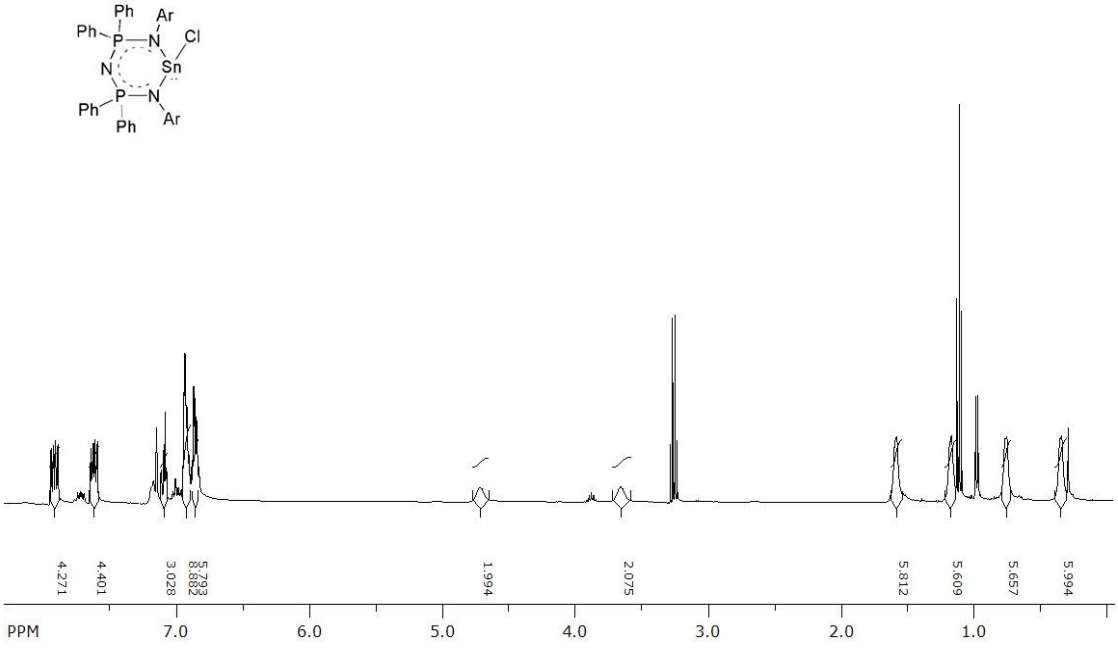

Fig. S27. ^{1}H NMR (400 MHz, C_6D_6) spectrum of $\mathbf{L_B}$SnCl **(7)**.

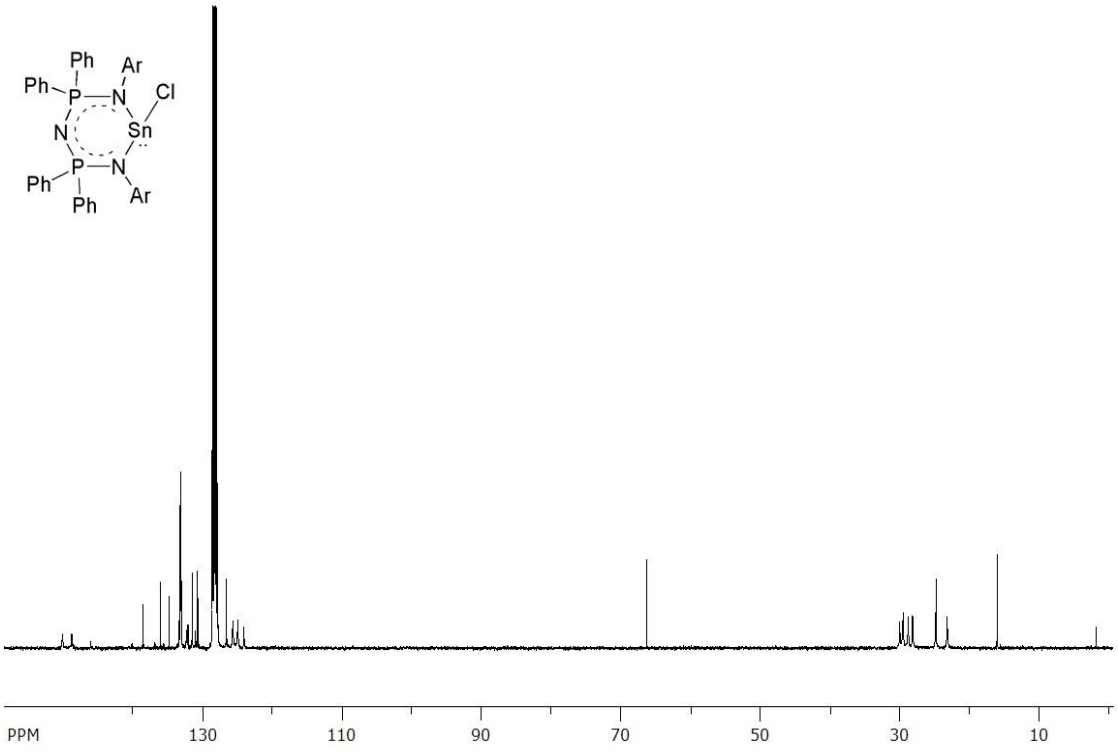

Fig. S28. ^{13}C NMR (100 MHz, C_6D_6) spectrum of $\mathbf{L_B}$SnCl **(7)**.

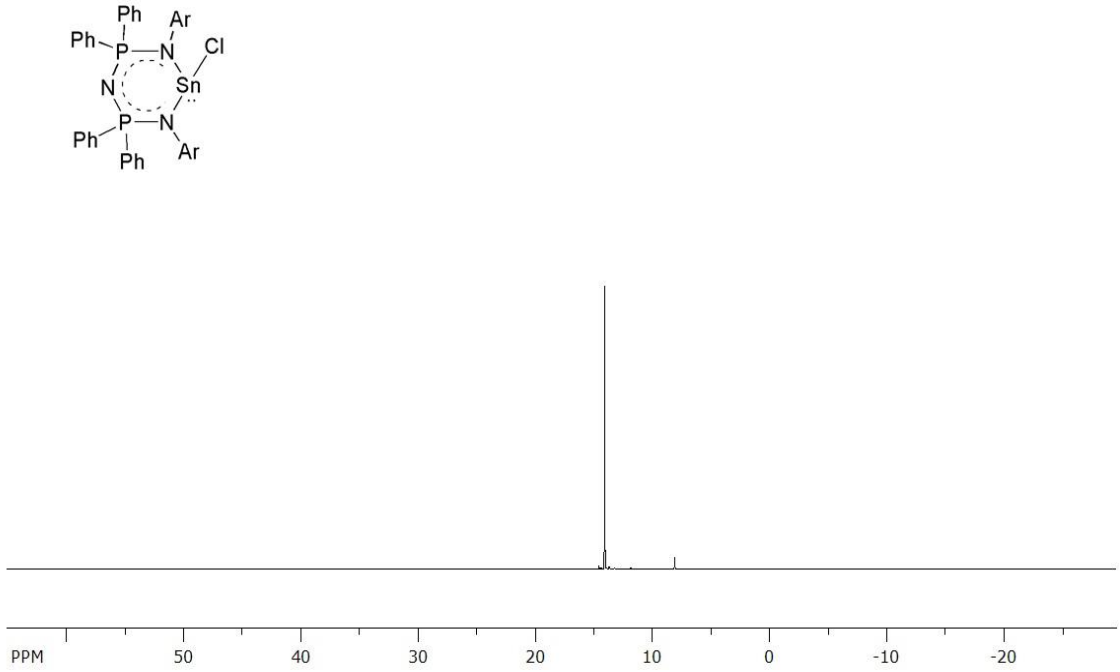

Fig. S29. $^{31}P\{^{1}H\}$ NMR (162 MHz, C_6D_6) spectrum of $\mathbf{L_B}$SnCl **(7)**.

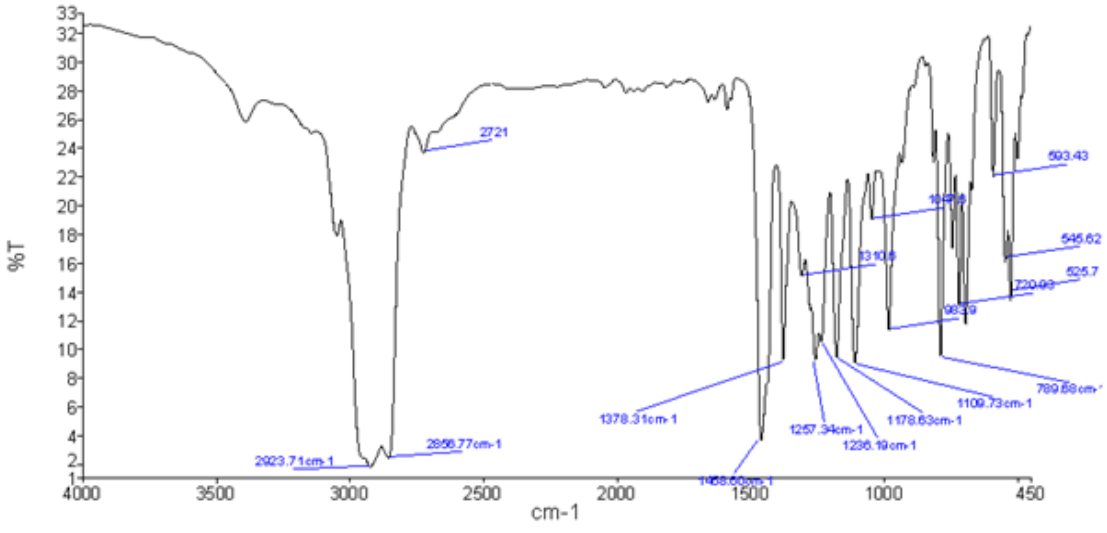

Fig. S30. IR spectrum of $\mathbf{L_B}$SnCl **(7)**.

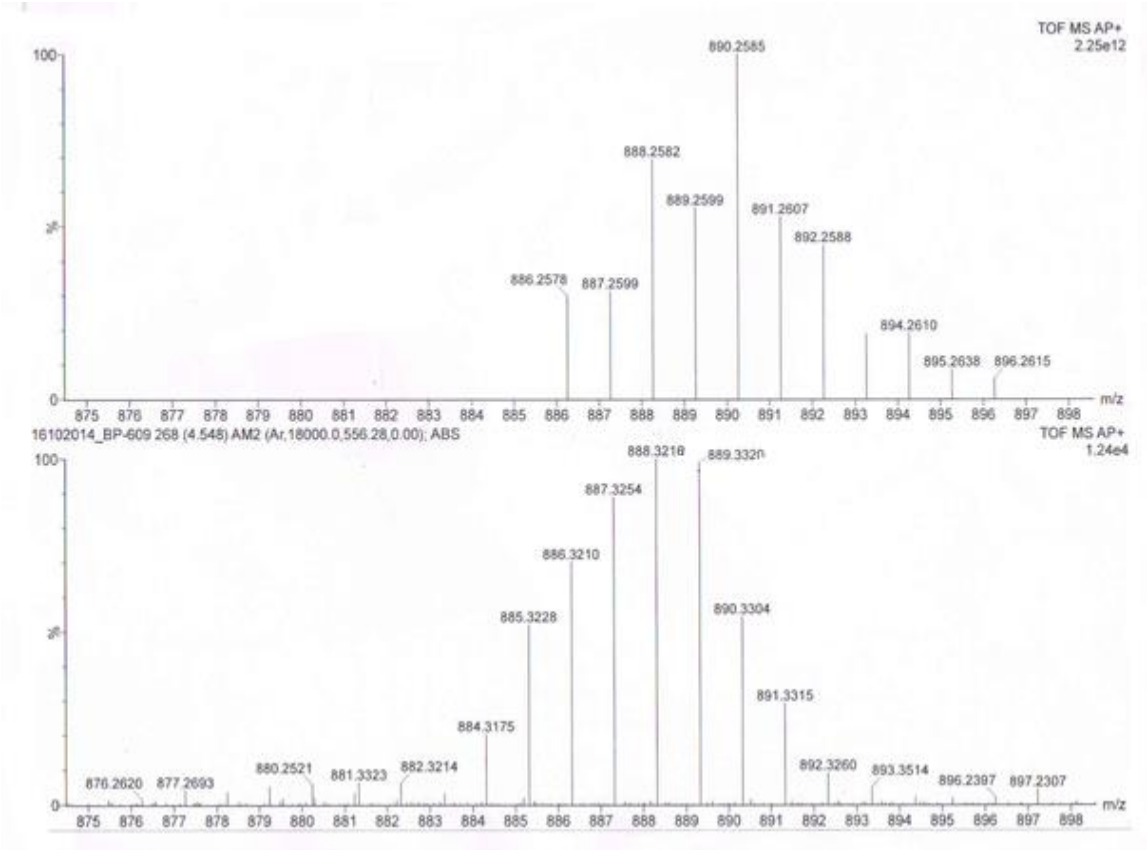

Fig. S31. Mass spectrum of $\mathbf{L_B}$SnCl **(7)**.

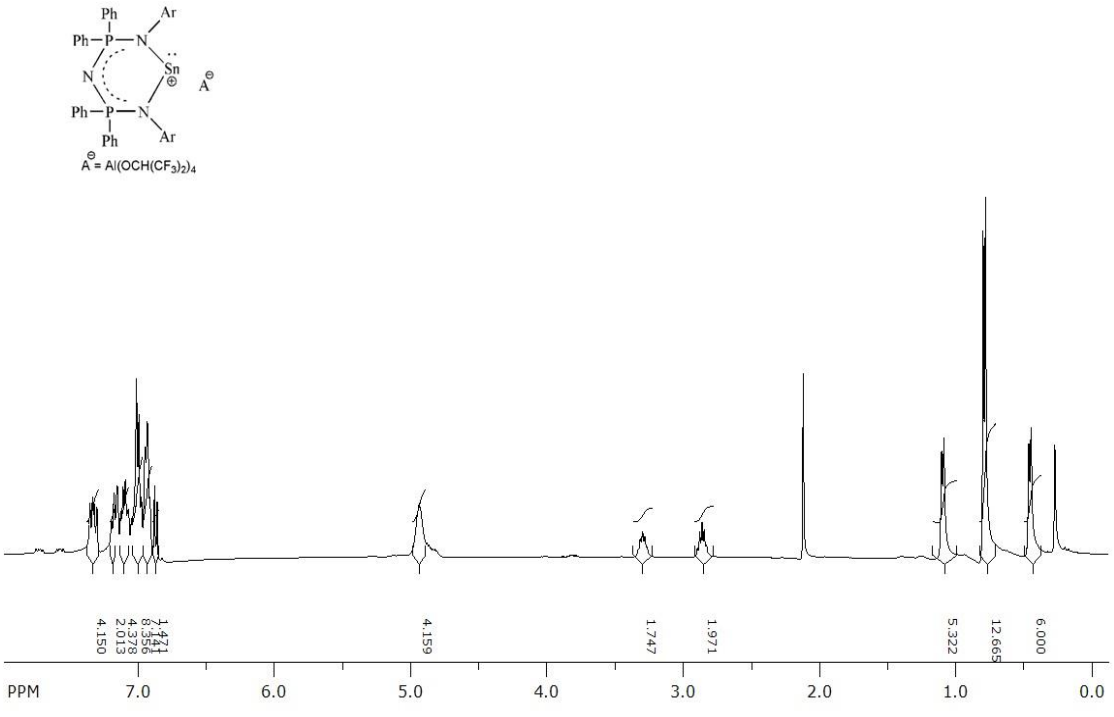

Fig. S32. ^{1}H NMR (400 MHz, C_6D_6) spectrum of $[\mathbf{L_B}Sn]^+[Al(OCH(CF_3)_2)_4]^-$ **(8)**.

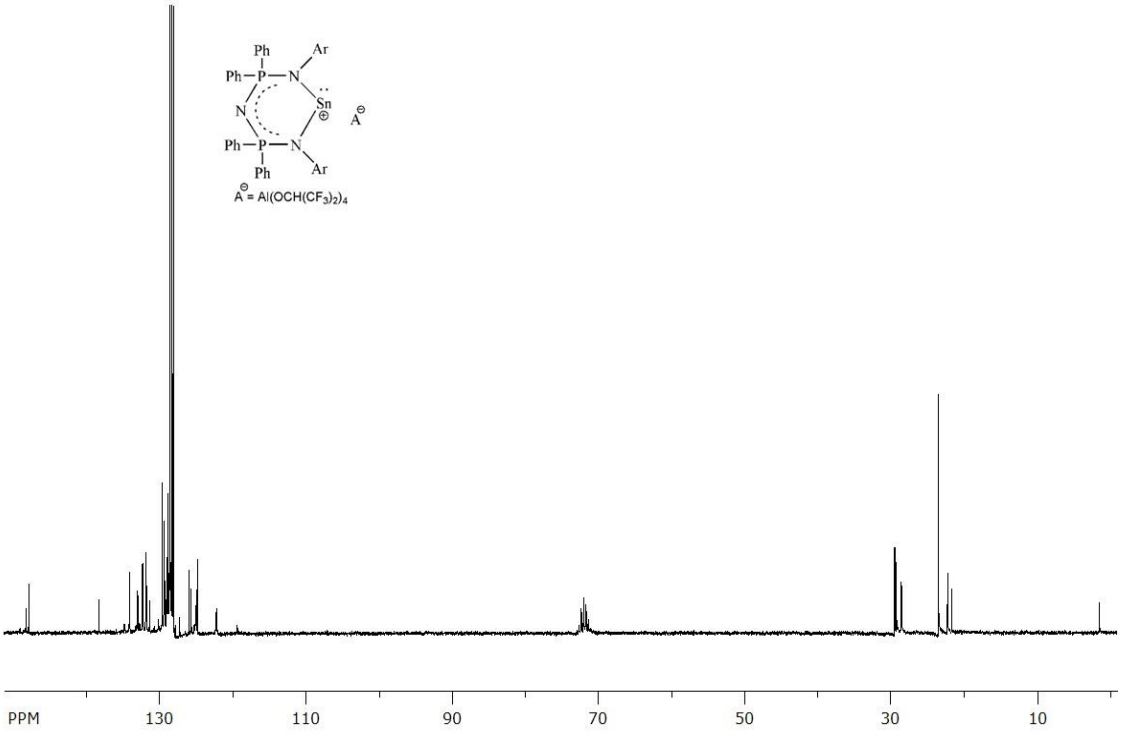

Fig. S33. ^{13}C NMR (100 MHz, C_6D_6) spectrum of $[\mathbf{L_B}Sn]^+[Al(OCH(CF_3)_2)_4]^-$ **(8)**.

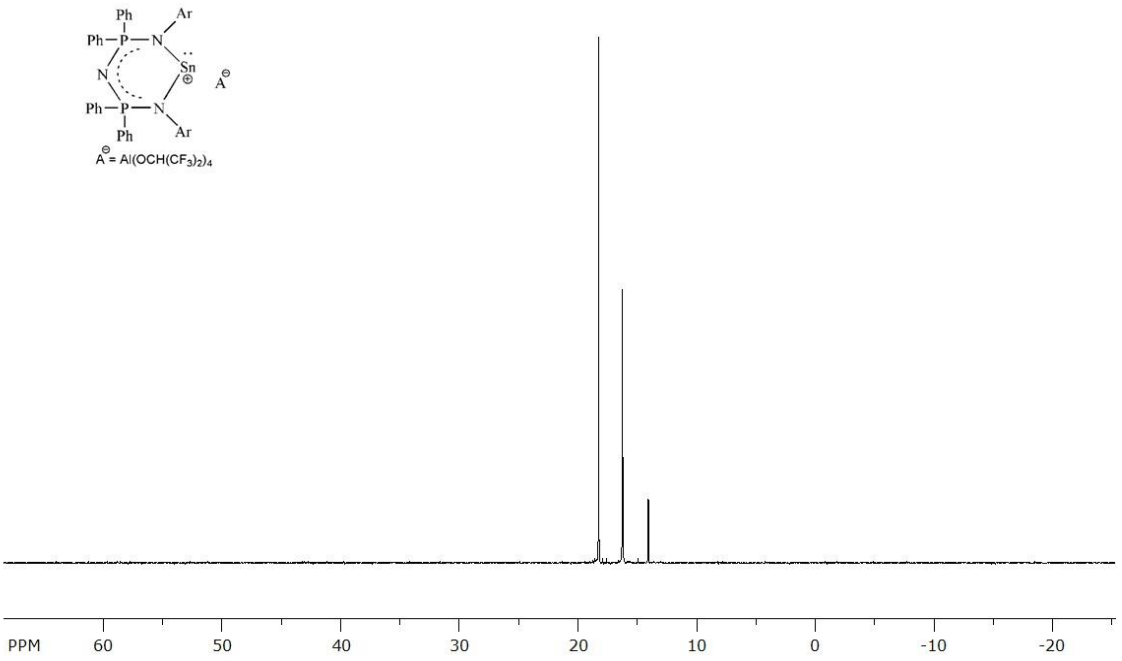

Fig. S34. $^{31}P\{^1H\}$ NMR (162 MHz, C_6D_6) spectrum of $[\mathbf{L_B}Sn]^+[Al(OCH(CF_3)_2)_4]^-$ **(8)**.

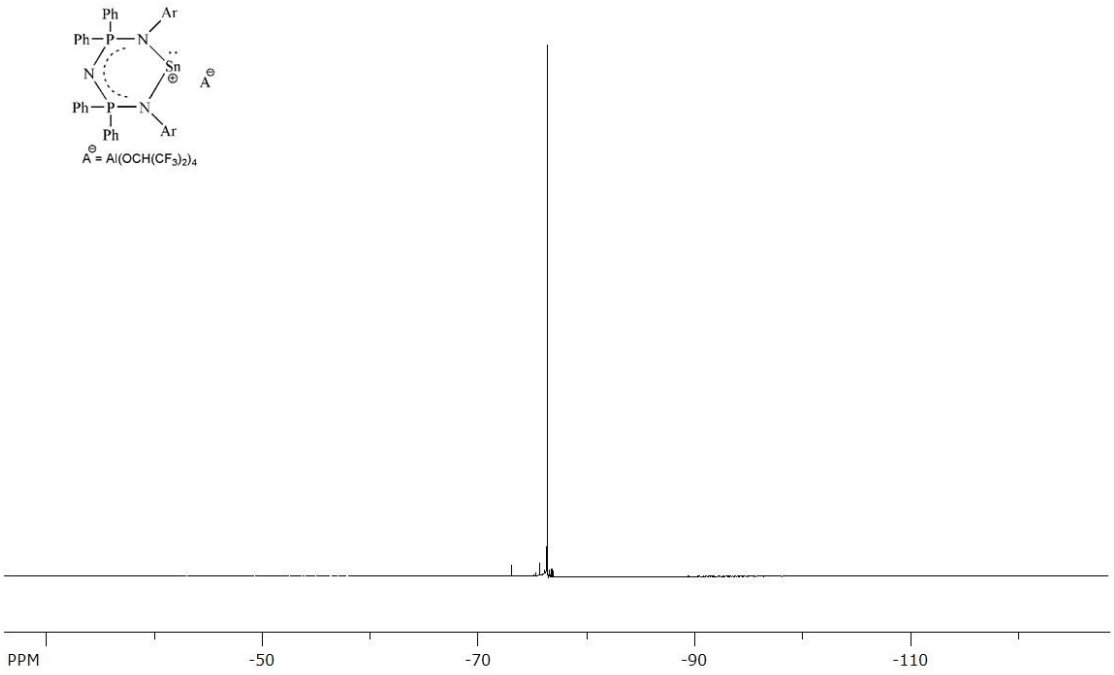

Fig. S35. ^{19}F NMR (376 MHz, C_6D_6) spectrum of $[\mathbf{L_B}Sn]^+[Al(OCH(CF_3)_2)_4]^-$ **(8)**.

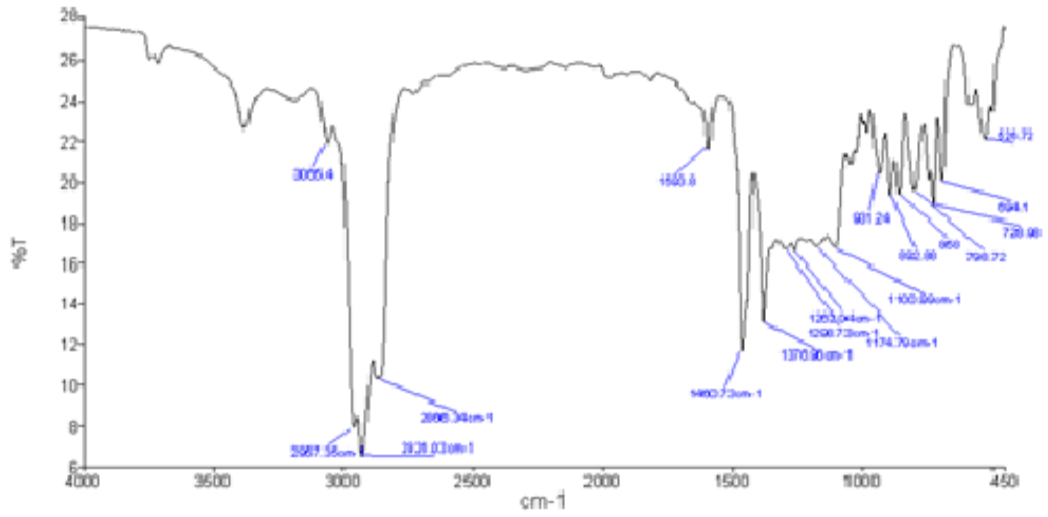

Fig. S36. IR spectrum of $[\mathbf{L_B}Sn]^+[Al(OCH(CF_3)_2)_4]^-$ **(8)**.

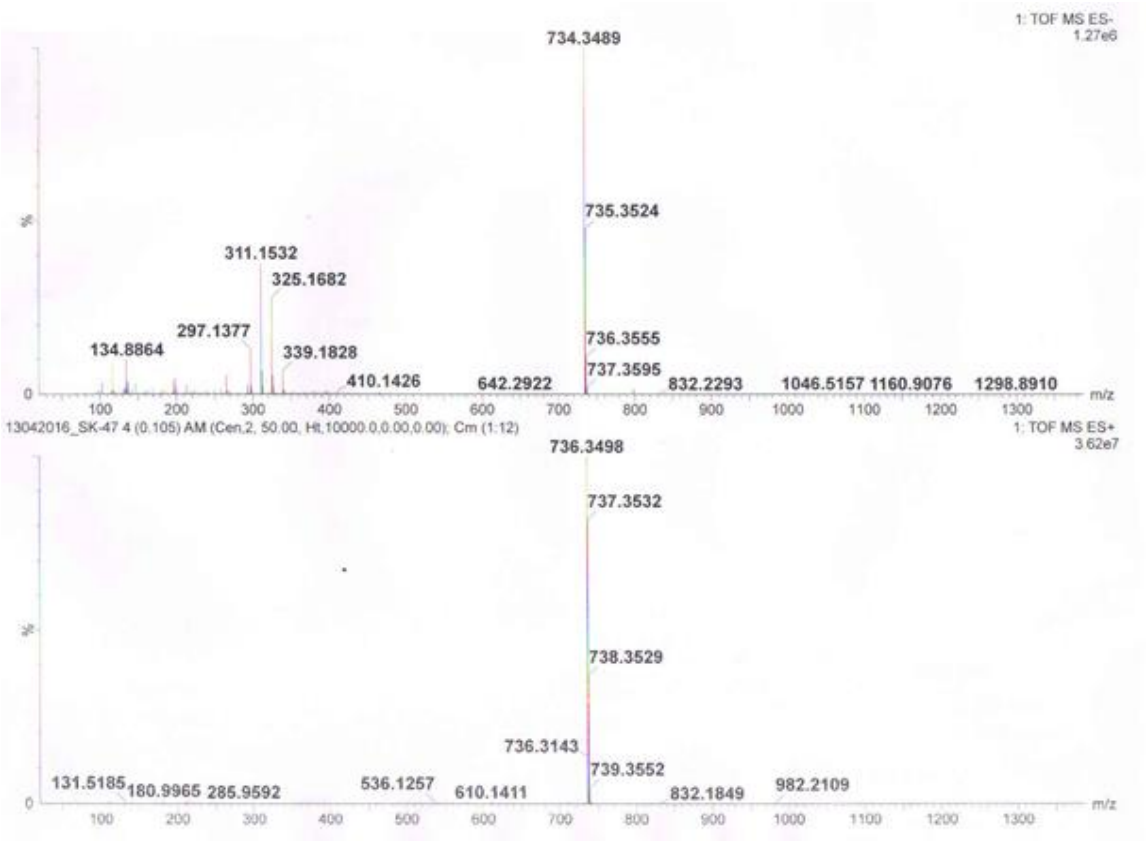

Fig. S37. Mass spectrum of $[\mathbf{L_B}Sn]^+[Al(OCH(CF_3)_2)_4]^-$ **(8)**.

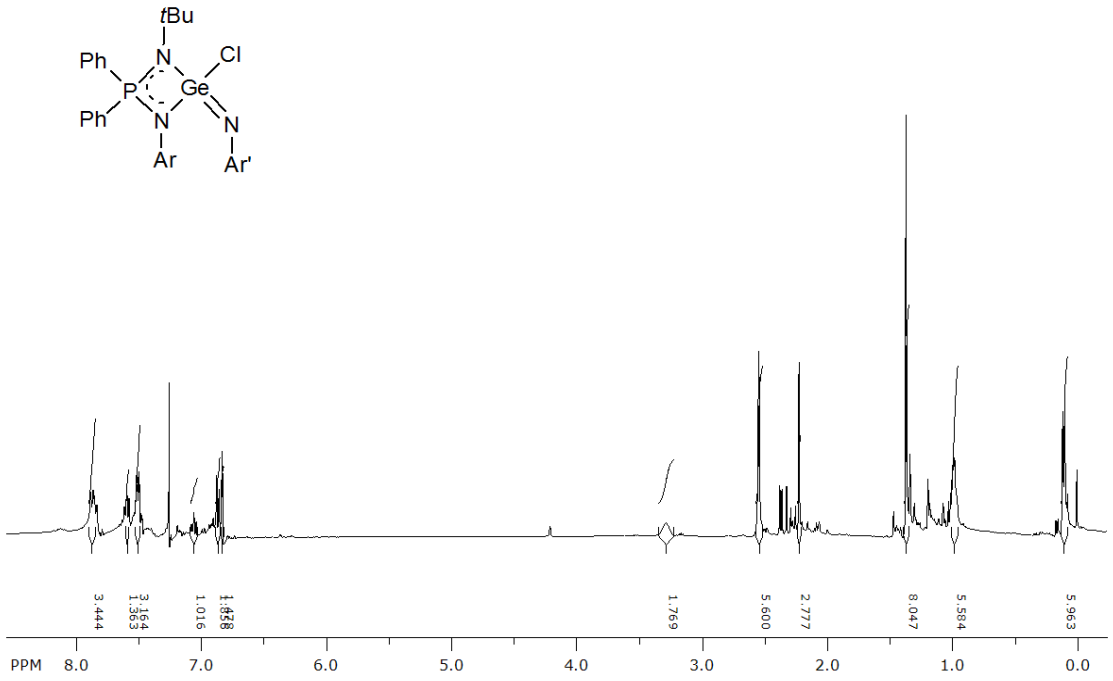

Fig. S38. ^{1}H NMR (400 MHz, $CDCl_3$) spectrum of $\mathbf{L_A}Ge(=NAr')Cl$ (Ar' = 2,4,6-$Me_3C_6H_2$) **(10)**.

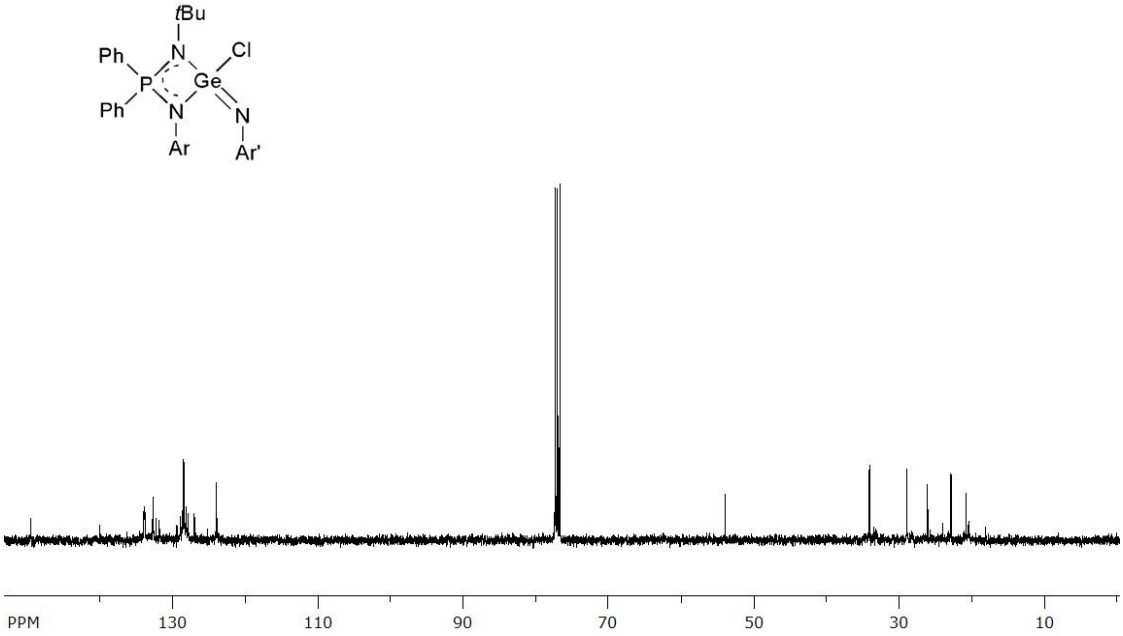

Fig. S39. ^{13}C NMR (100 MHz, $CDCl_3$) spectrum of

L_AGe(=NAr')Cl (Ar' = 2,4,6-$Me_3C_6H_2$) **(10)**.

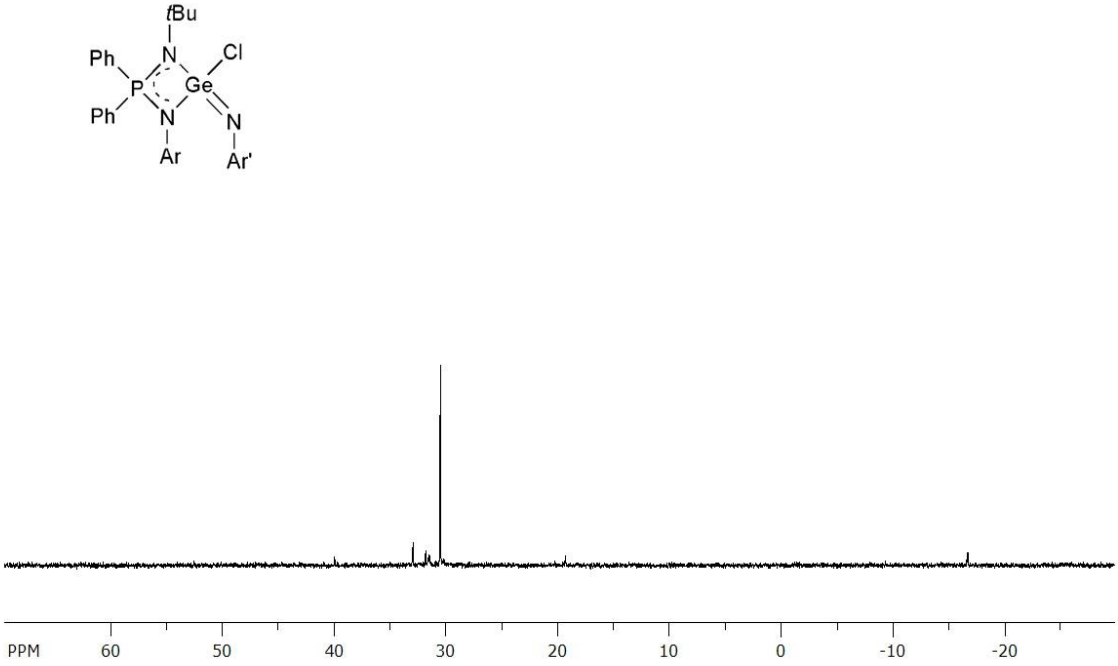

Fig. S40. $^{31}P\{^1H\}$ NMR (162 MHz, $CDCl_3$) spectrum of

L_AGe(=NAr')Cl (Ar' = 2,4,6-$Me_3C_6H_2$) **(10)**.

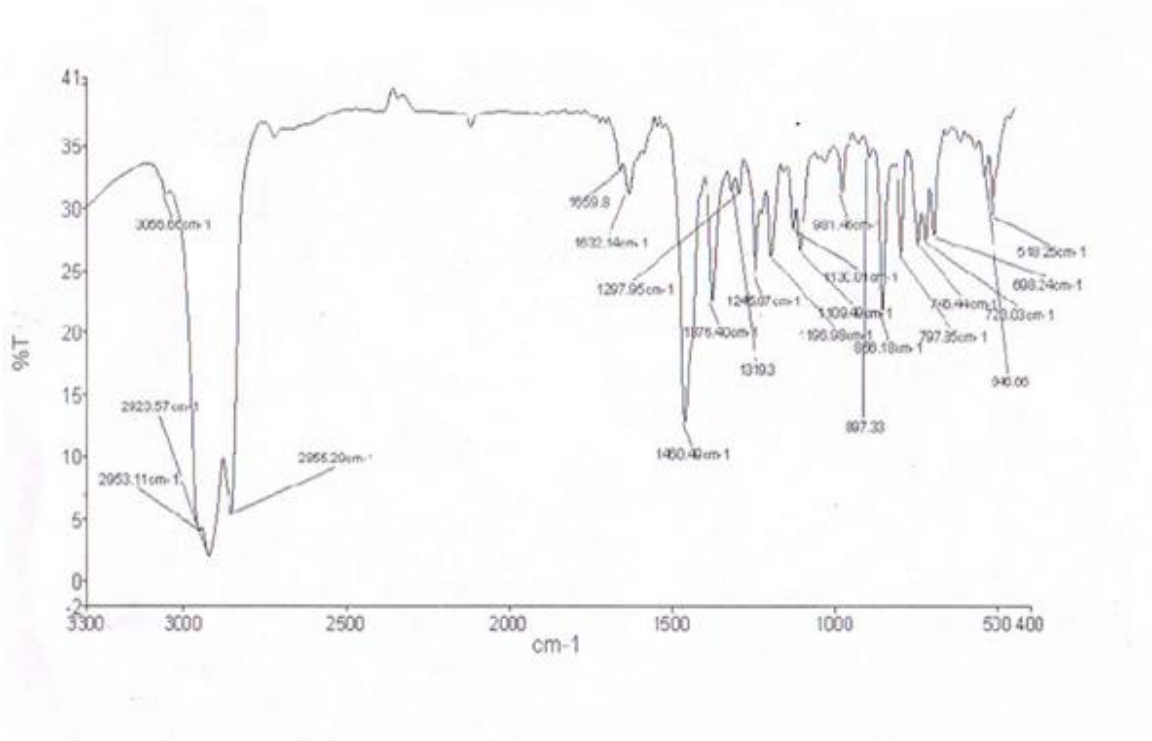

Fig. S41. IR spectrum of $\mathbf{L_A}$Ge(=NAr')Cl (Ar' = 2,4,6-$Me_3C_6H_2$) **(10)**.

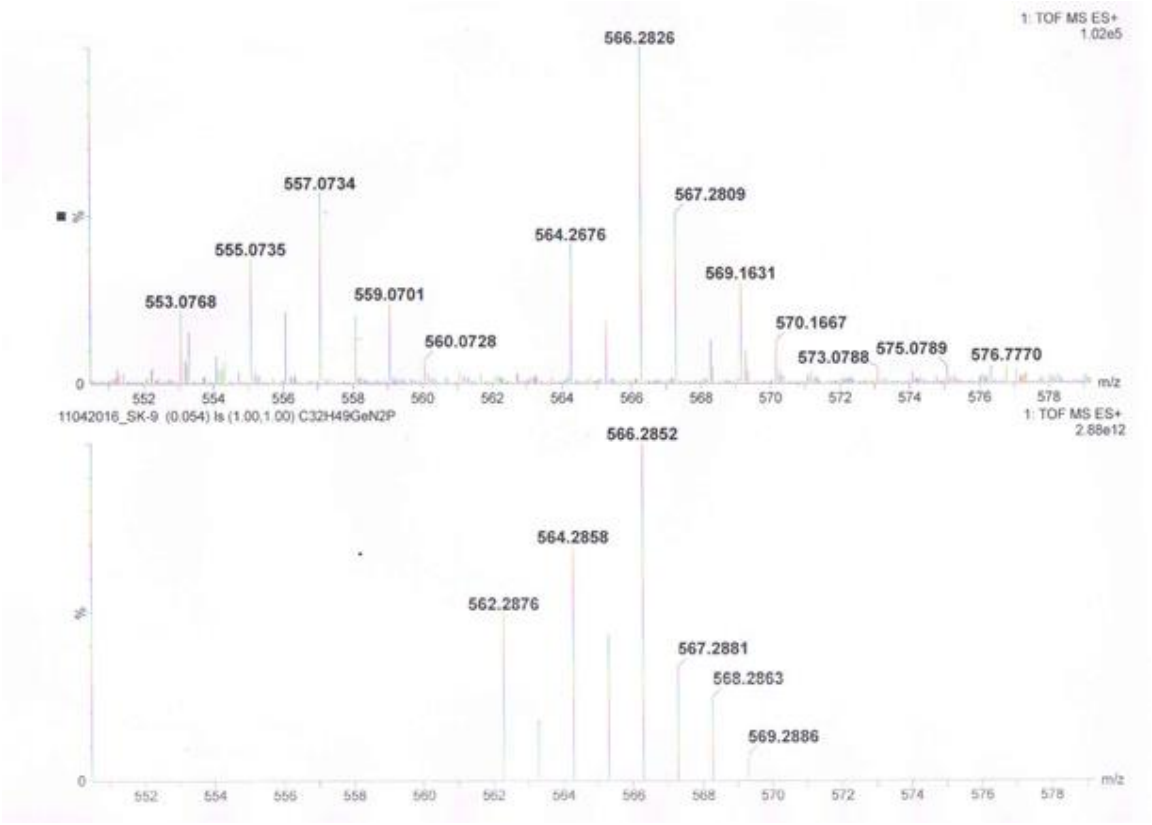

Fig. S42. Mass spectrum of $\mathbf{L_A}$Ge(=NAr')Cl (Ar' = 2,4,6-$Me_3C_6H_2$) **(10)**.